「ひので」による理解の到達点

横山央明
東京大学地球惑星

参考文献

SOLAR-B衛星提案書 1996年11月
「ひので」プロジェクトミッション期間延長提案書 2011年3月
「ひので」プロジェクトミッション期間延長提案書 2013年5月

Table of contents

Overview of Hinode results & What to do next.

- Chromospheric dynamics
- Flares: flows and triggers
- Coronal heating and solar wind
- Photospheric magnetism and flows

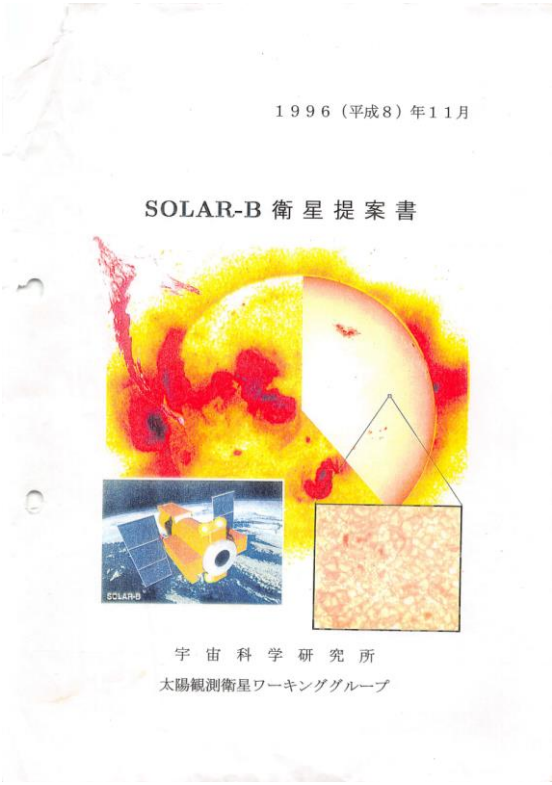

SOLAR-B衛星提案書1996年11月

挑戦する研究課題

- 外層大気（コロナ・彩層）の加熱メカニズム
- 太陽磁場の基本構造としての微細磁束管とダイナモ機構
- コロナのダイナミックスとリコネクションの詳細究明

Chromospheric dynamics

Coronal transverse waves in a prominence

Okamoto+ 2007

fine-scale threadlike structures oscillating in the plane of the sky with periods of several minutes

Alfven waves

(c.f. Ofman & Wang 2008)

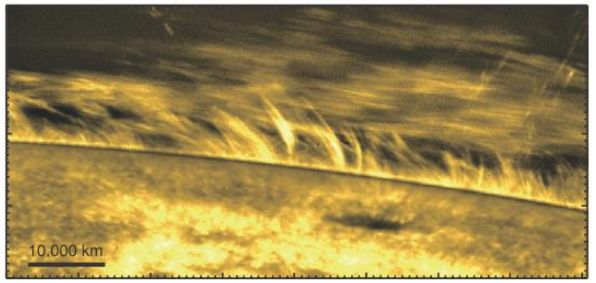

Fig. 1. High-resolution image on the solar limb obtained with SOT aboard Hinode. This observation was performed with a cadence of 15 s from 19:33 to 20:44 UT on 9 November 2006. Tick marks have a spacing of 1000 km on the Sun. A radial density filter is applied to show the brighter photosphere and the fainter coronal structures in the same image. The main sunspot of NOAA AR 10921 as well as the trailing bright plage areas are visible on the disk. Above the limb, ubiquitous vertical spicules are seen below the horizontal threads of the AR prominence. The cloudlike prominence structure is located 10,000 to 20,000 km above the visible limb and exhibits a very complex fine structure with predominant horizontal threadlike features. The intensity of the prominence in Ca II H-line radiation is about 1% of the on-disk photosphere.

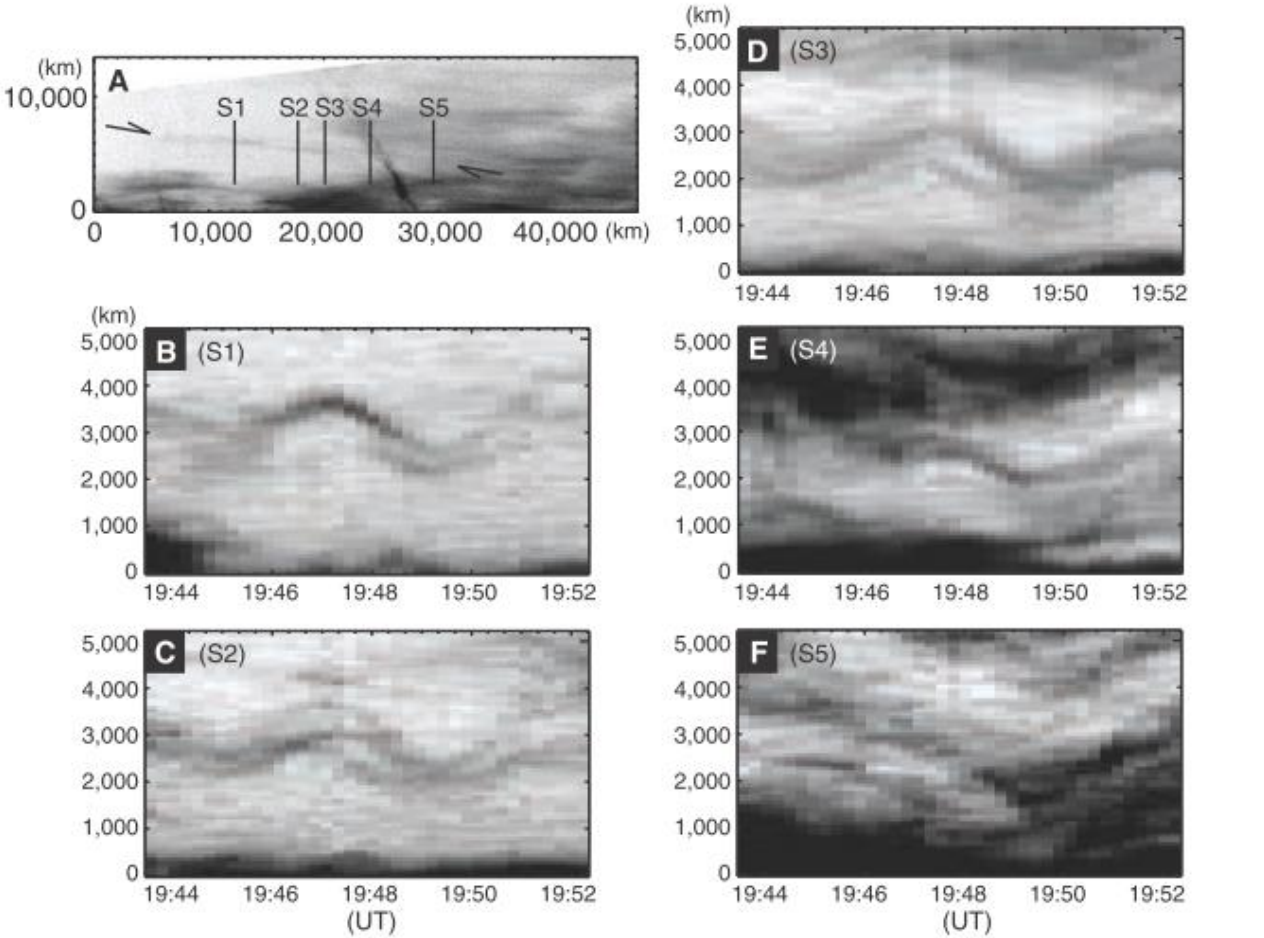

Fig. 3. Example of a prominence thread undergoing synchronous oscillation along its entire length. **(A)** The long thread extending ~16,000 km. Lines S1 to S5 indicate the locations of height versus time plots shown in (B to F). The arrows indicate both sides of the long thread oscillating synchronously. **(B to F)** Height-time plots (shown in negative contrast) for the locations indicated in (A). Maximum and minimum amplitudes occur at nearly the same time for all locations.

Chromospheric Alfvenic Waves

De Pontieu+ 2007

Alfven waves with amplitudes on the order of 10 to 25 km/s and periods of 100 to 500 sec.

energetic enough to accelerate the solar wind and possibly to heat the quiet corona

(c.f. Okamoto & Depontieu 2011)

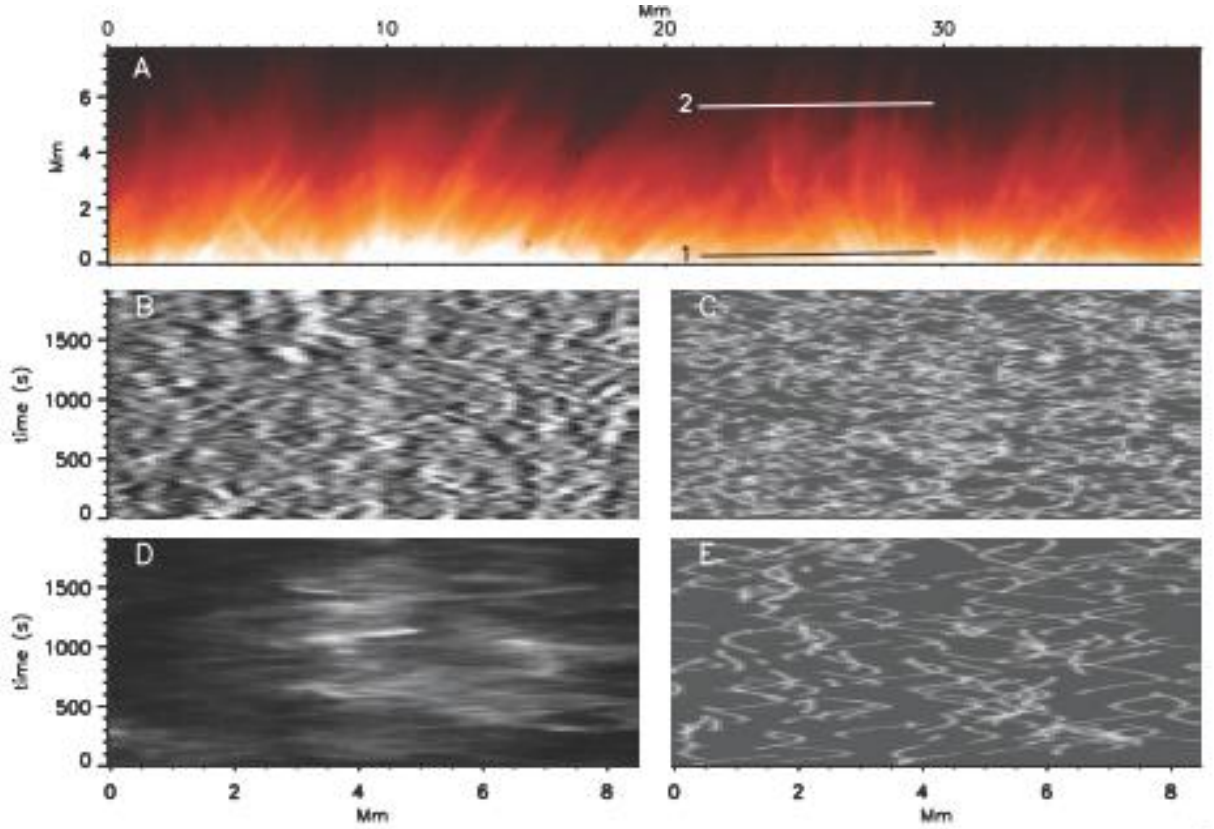

Fig. 2. Illustration of the ubiquity of Alfvén waves in the chromosphere. (**A**) A Hinode SOT Ca II H 3968 Å image showing how thin spicules that outline the magnetic field dominate the chromosphere. (**B**) A space-time plot [along the cut labeled 1 in (A)] of the Ca intensity processed to enhance 200-km-wide structures. The plot is dominated by a multitude of criss-crossed short linear tracks caused by spicular motion transverse to the magnetic field direction. (**D**) A similar cut for the line labeled 2 in (A). Image enhancement is unnecessary at these heights because of the smaller number of spicules. Similar linear tracks are visible, as well as swings. The general characteristics (linear tracks and swings) of (B) and (D) are well reproduced by cuts that are generated from Monte Carlo simulations [(**C**) and (**E**)] (*12*) in which spicules carry Alfvén waves.

Chromospheric Anemone Jets

(Shibata et al. 2007; Nishizuka et al. 2011; talk by Singh et al. ST01-A005)

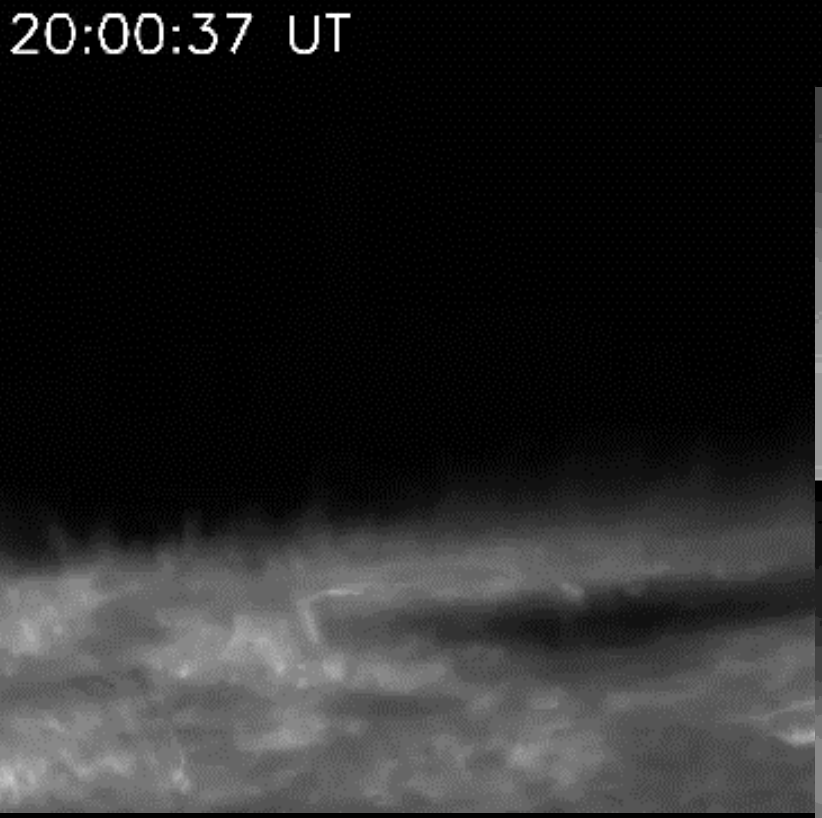

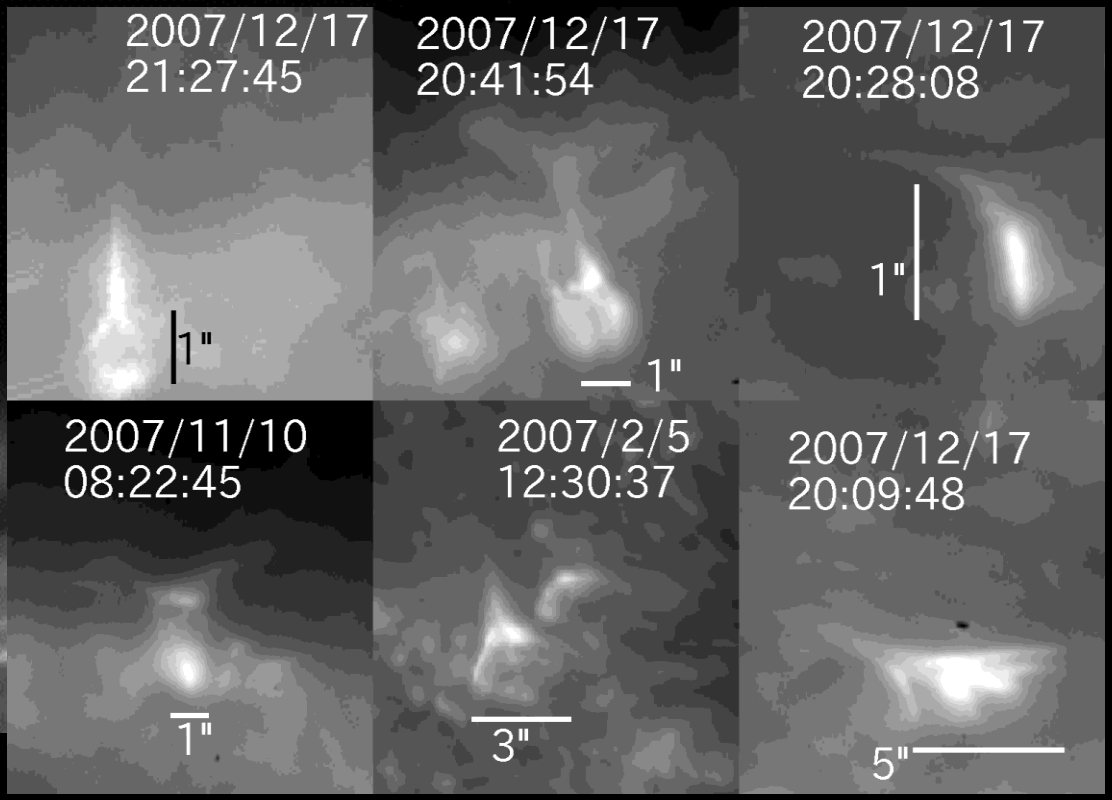

Found in active regions
Cusp-shaped structure and bright footpoint
length 1-4 Mm, lifetime 100-500s
velocity 5-20km/s ~local Alfven speed

Penumbral micro-jets

(Katsukawa et al. 2007; Jurcak & Katsukawa 2008; 2010; poster by Katsukawa ST01-A004)

Ca II H movie

FFT filtered (f>3mHz)

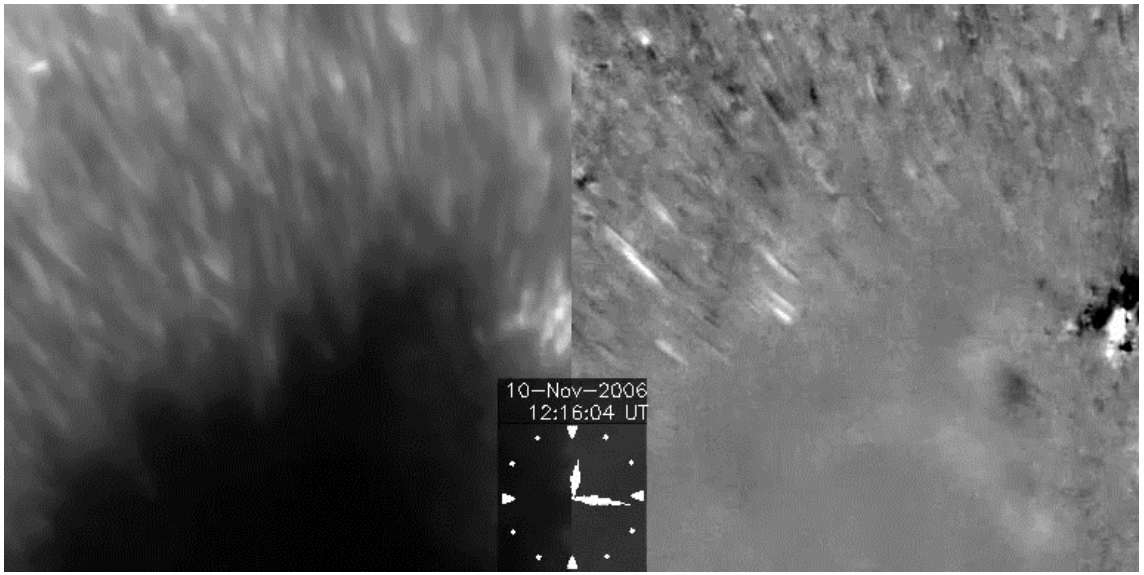

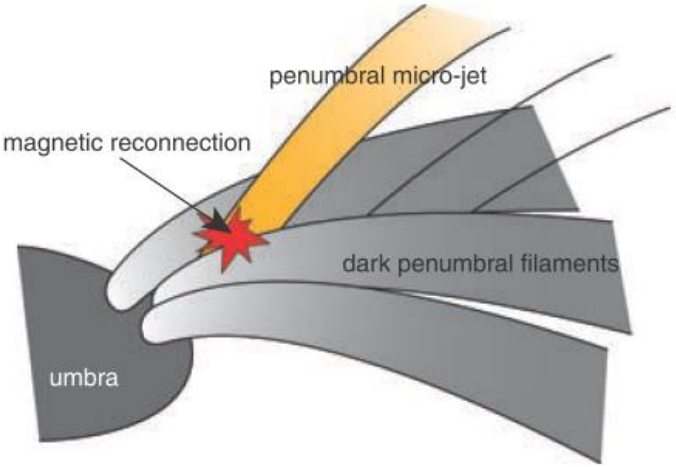

- Small scale jet-like features are discovered in the penumbral chromosphere.
- Length: 1000 - 4000km, Duration: Shorter than 1 min
- velocity > several 10s km/s, beyond the sound speed (~10km/s)
- Observed everywhere above the penumbra
- following the orientation of the background field
- Corresponding downflows

Quiescent prominence dynamics

Berger+ 2008; 2010

filamentary downflows and vortices

dark, episodic upflows: 170-700 km in width, exhibit turbulent flow and rise with constant speeds of 20km/s from the base to heights of 10-20 Mm. resemble buoyant starting plumes

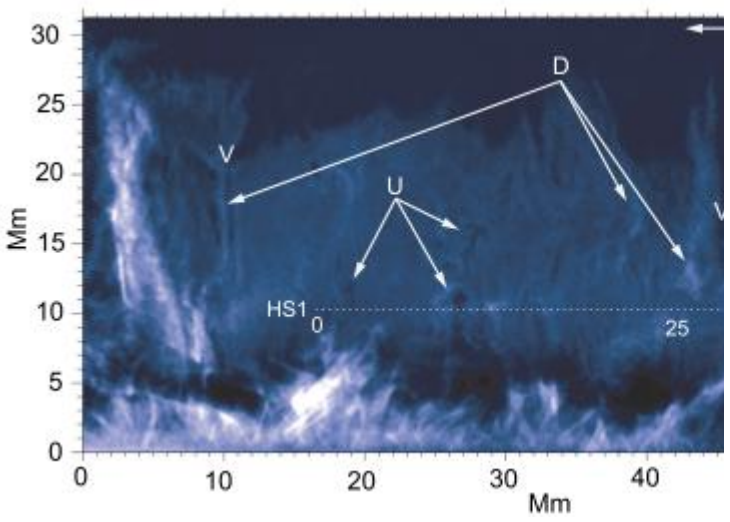

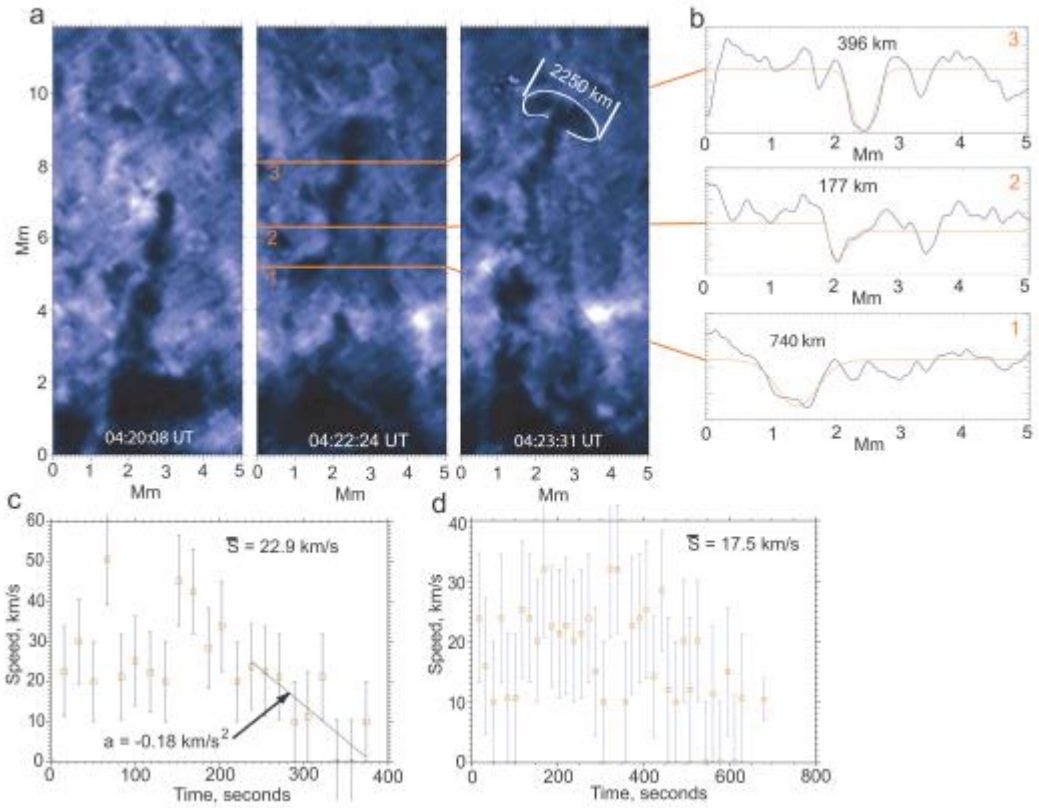

Chromospheric dynamics: summary

Waves

Transverse waves found in prominences (Okamoto+ 2007), spicules (De Pontieu+ 2007), photospheric flux tubes (Fujimura & Tsuneta 2009), jets (Nishizuka+ 2008)...

Evidence of the resonant-absorption thermalization (Okamoto+ 2007)

Chromospheric reconnection

Anemone jets (Shibata+ 2007), penumbral micro-jets (Katsukawa+ 2007)

→ Ubiquitousness of magnetic reconnection, magnetic reconnection in partially ionized plasmas (e.g. Leake+ 2013), and/or in partial-component asymmetric (e.g. Nakamura+ 2012)

Spicules

“Type-I”, “Type-II” (mis?)understanding (De Pontieu+ 2007; Zhang+ 2012)

→ need further study for mechanism

Prominence internal flows

Turbulent flows inside (Berger+ 2008; 2010)

→ Magnetic Rayleigh-Taylor instability (Hillier+ 2012)

Flares and coronal activity

Flare loop flows

Yokoyama & Shibata 2001

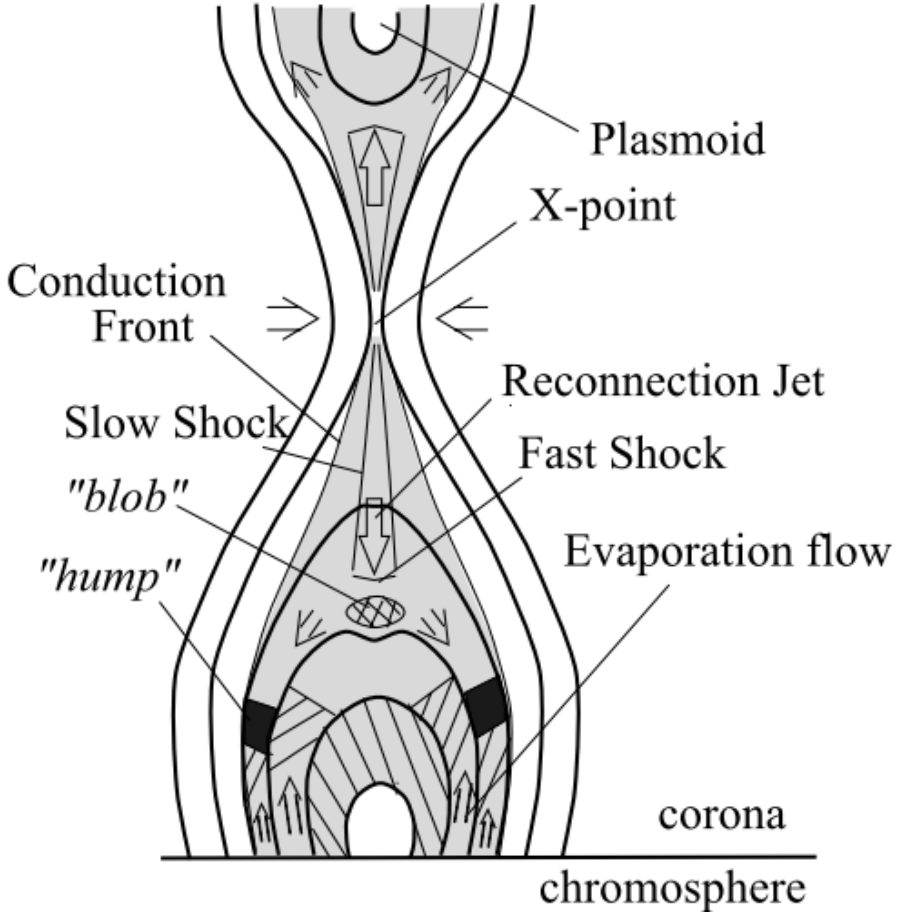

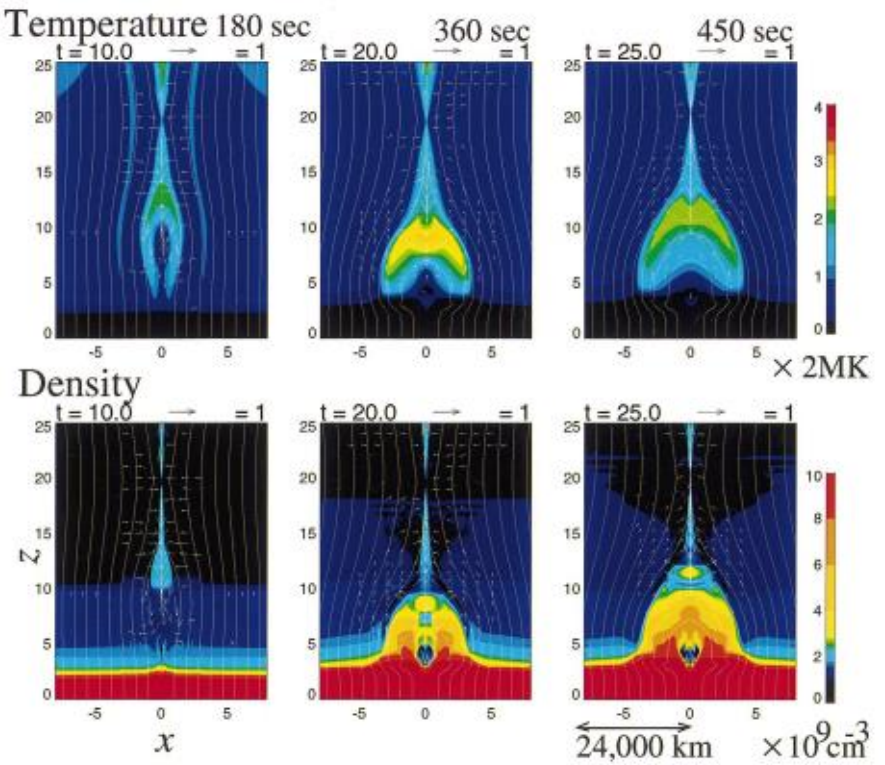

Reconnection flows in a flare

Hara+ 2011

- Loop top hot source: 12MK, 1e10/cm^3, dV~100km/s, V~30km/s
- a fast jet nearby: 200km/s: V>200km/s
- inflow: 1.2MK, 2.5e9/cm^3, 20 km/s
- reconnection rate 0.05-0.1

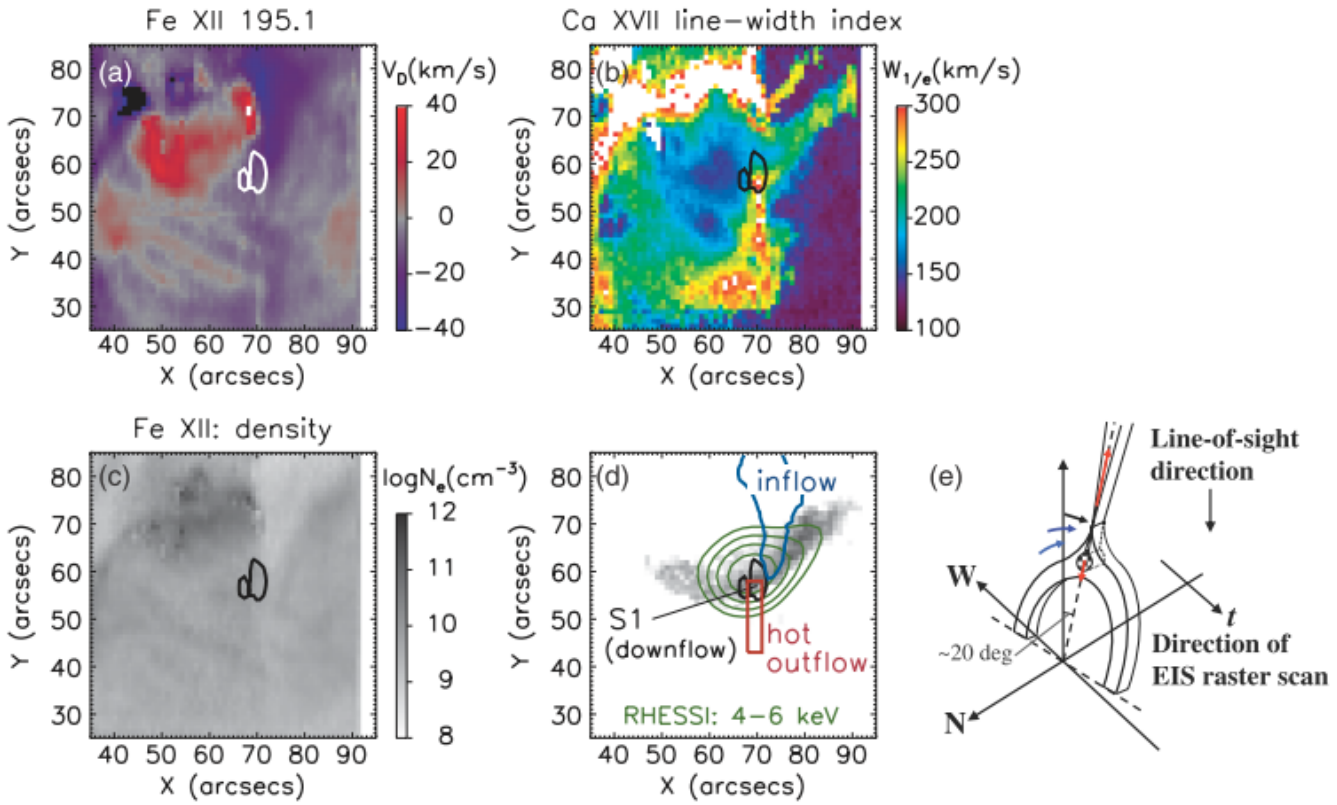

Magnetic field structures triggering flares

Kusano+ 2012

two types of small mag. structures favor the onset of eruptions

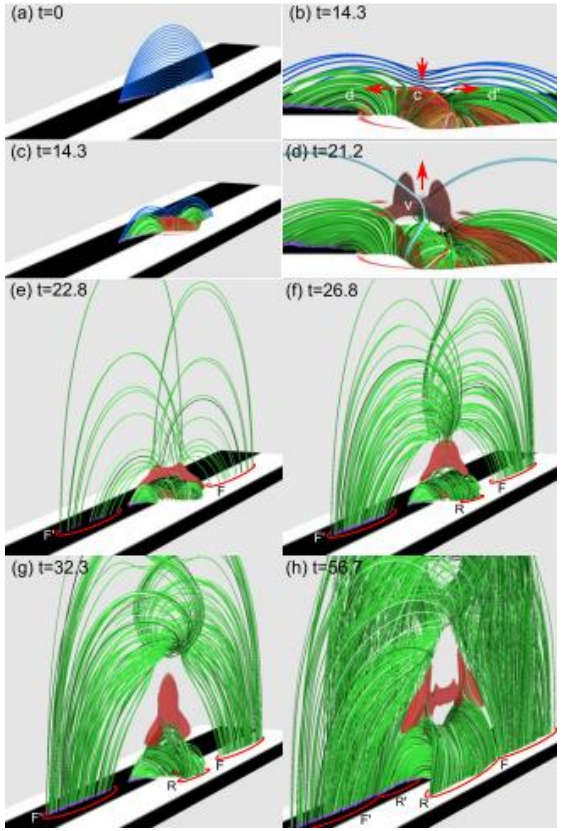

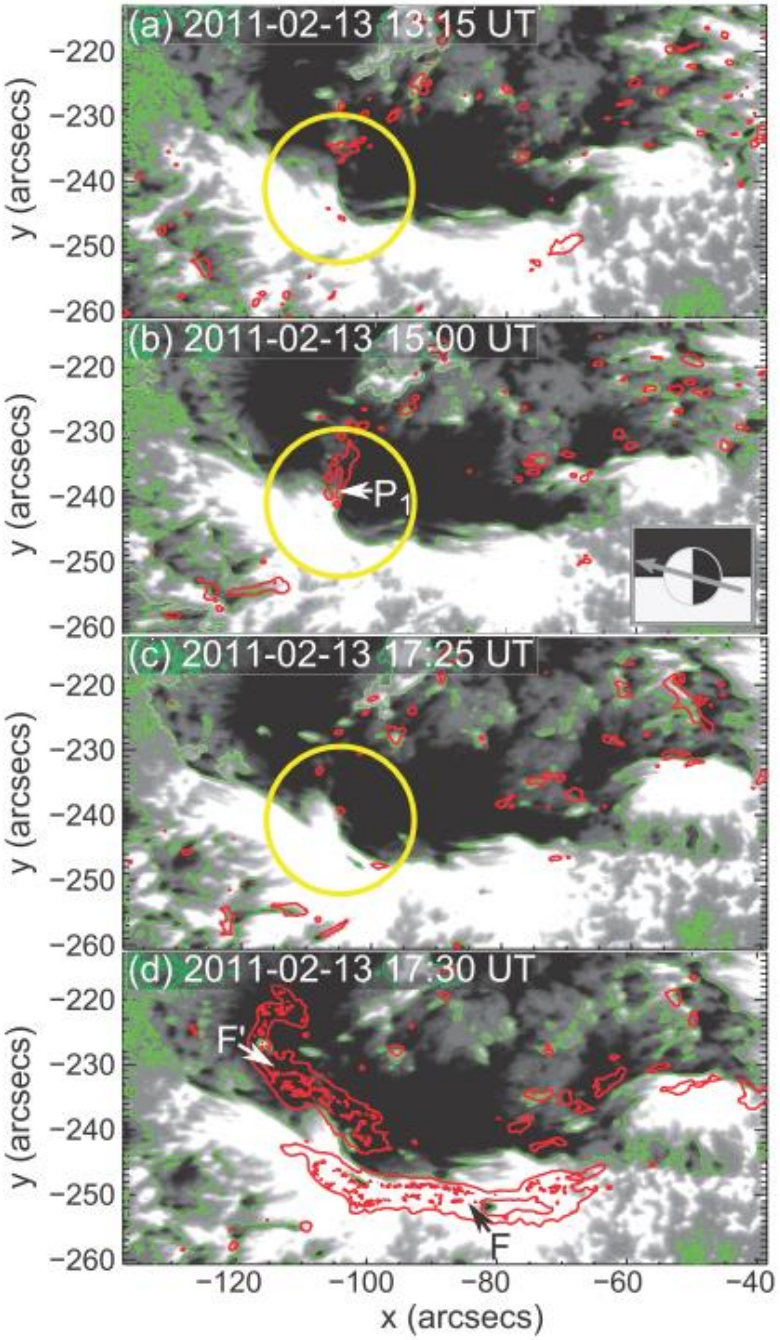

Alfven waves in solar X-ray jets

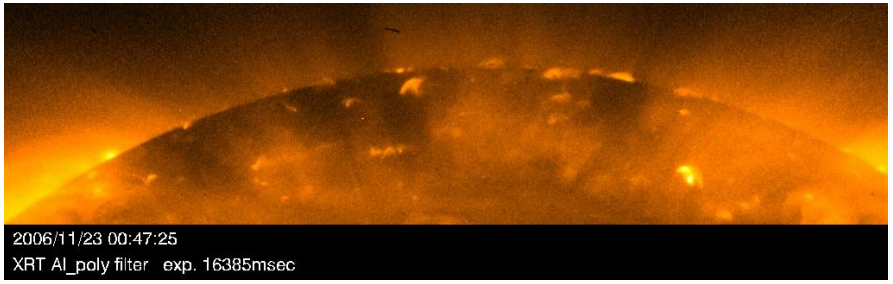

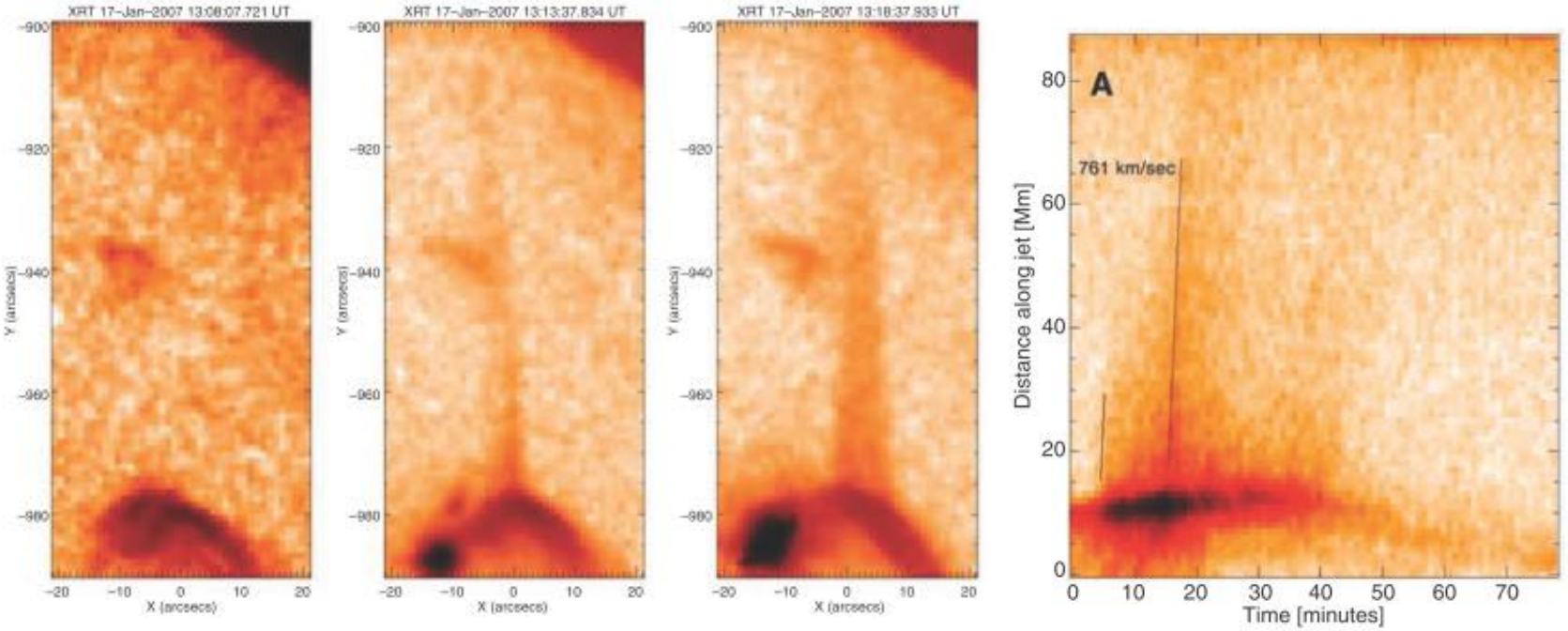

Cirtain+ 2007

- x-ray jets have two distinct velocities: one near the Alfven speed (~ 800km/s) and another near the sound speed (200km/s)

Flares and coronal activities: summary

Flows

Reconnection outflows & inflows observed (Hara+ 2011; 2014)

Shocks not yet.

(SDO/AIA observations; e.g., Takasao+ 2012; Su+ 2013)

Nonthermal aspects

→ not so much addressed yet (e.g. Minoshima+ 2009)

Trigger

Kusano+'s (2012) model, Observationally supporting evidence (Bamba+ 2013; Toriumi+ 2014)

→ Not sufficient condition ? Sigmoids unrelated ?

Force-free modeling of active region magnetic field

→ Issues became clear: photosphere-to-corona interfaces (DeRosa+ 2009; Schrijver+ 2008)

Coronal heating and solar wind

Coronal heating: 1D simulations

Antolin+ 2008

(c.f. Moriyasu+ 2004)

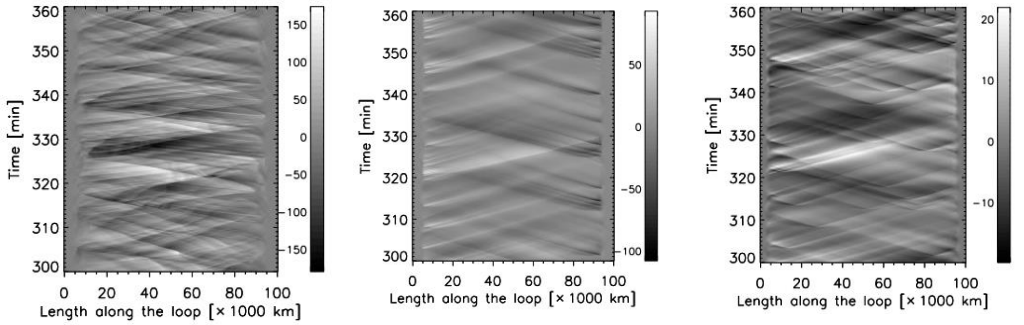

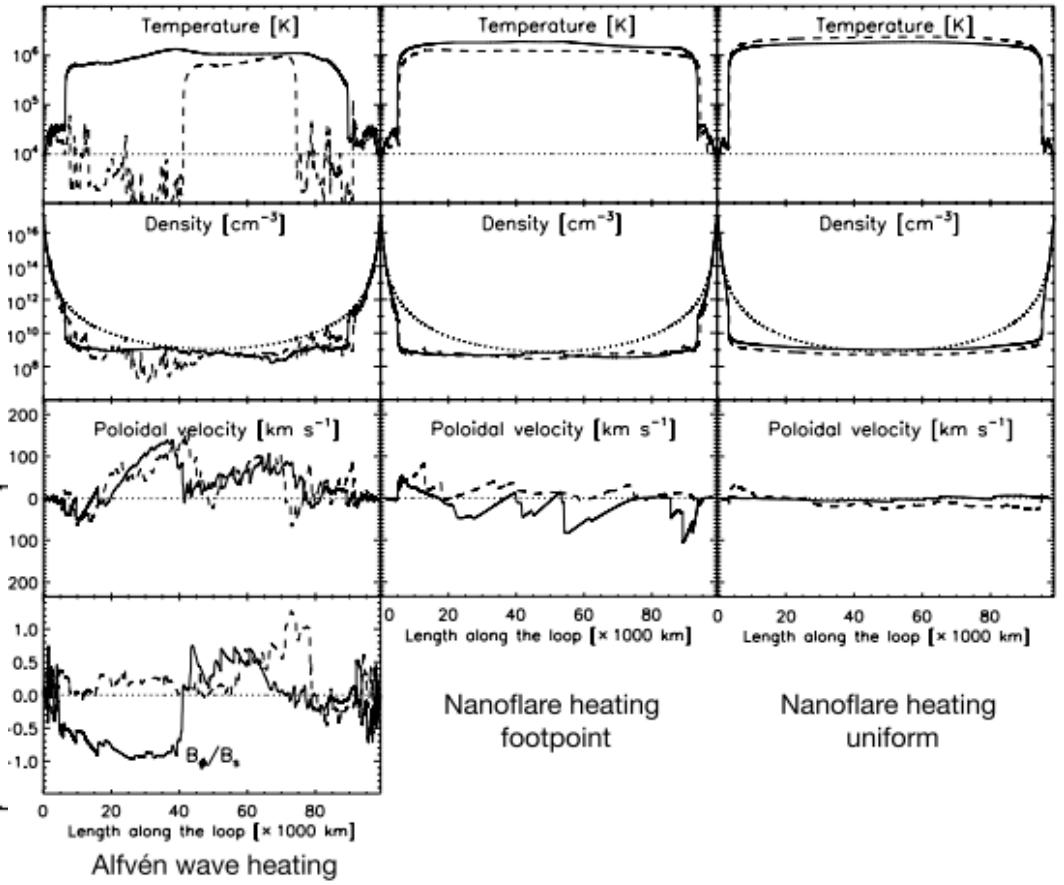

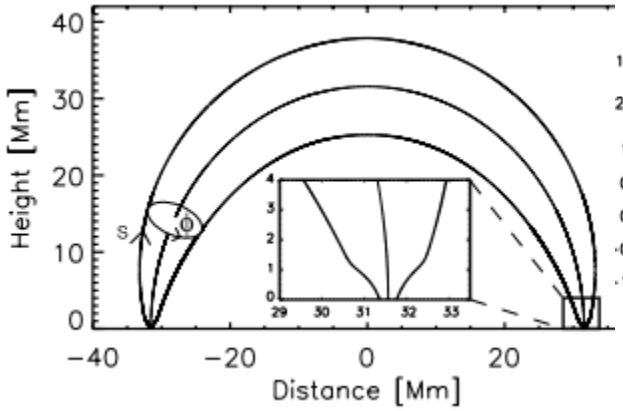

Alfven wave heating model

Suzuki & Inutsuka 2005; Matsumoto & Suzuki 2012

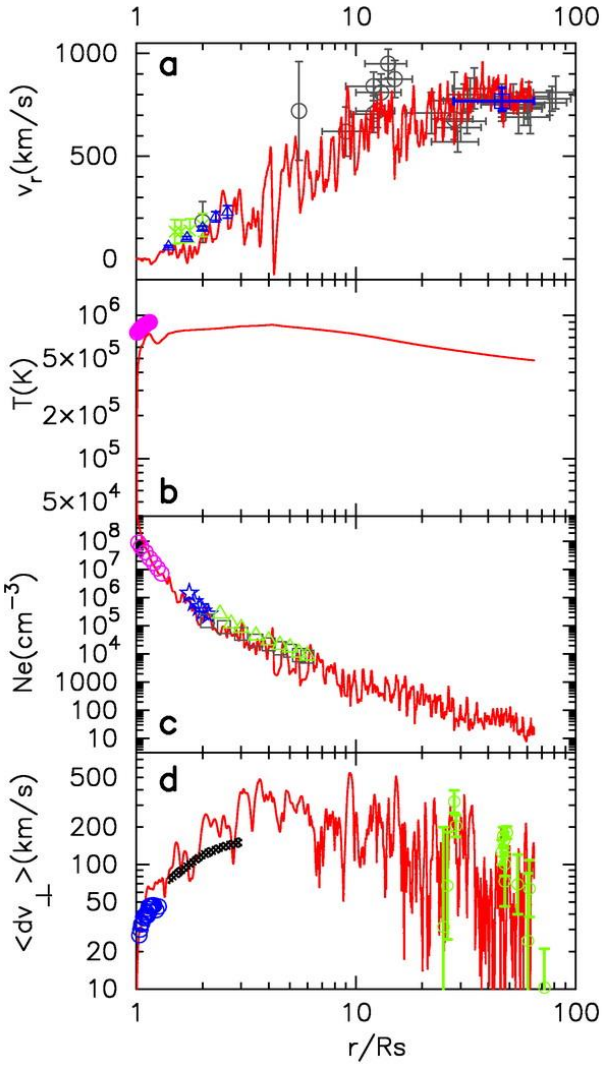

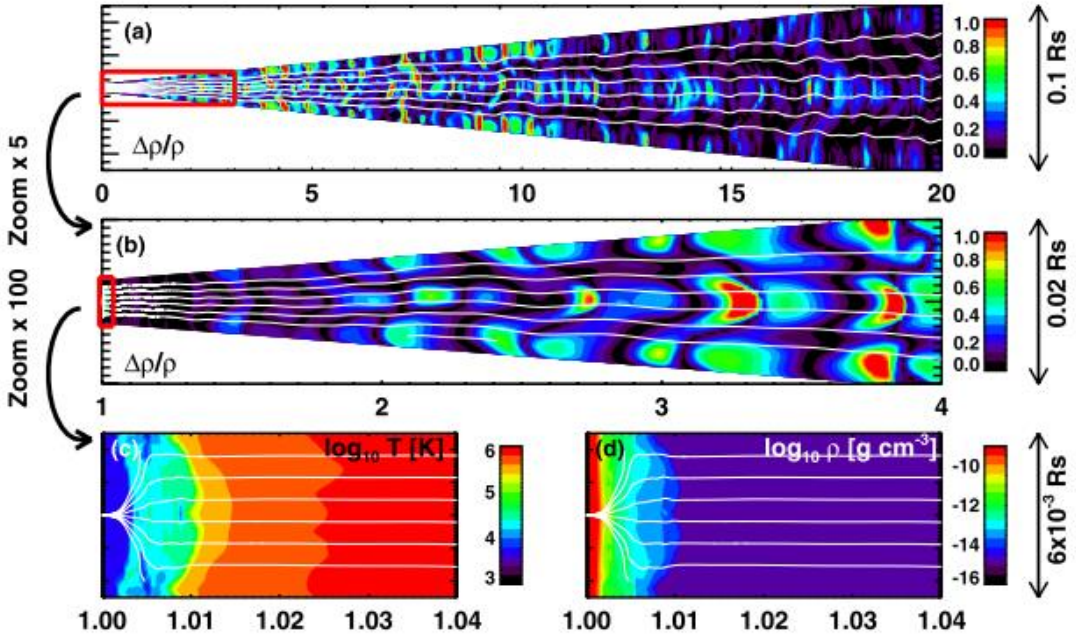

Motions in EUV coronal loops

Hara+ 2008

-- upflow motions of tens of km/s and enhanced nonthermal velocities near the footpoints

-- near the limb, both upflows and nonthermal velocities decrease

-- suggest unresolved high-speed upflows

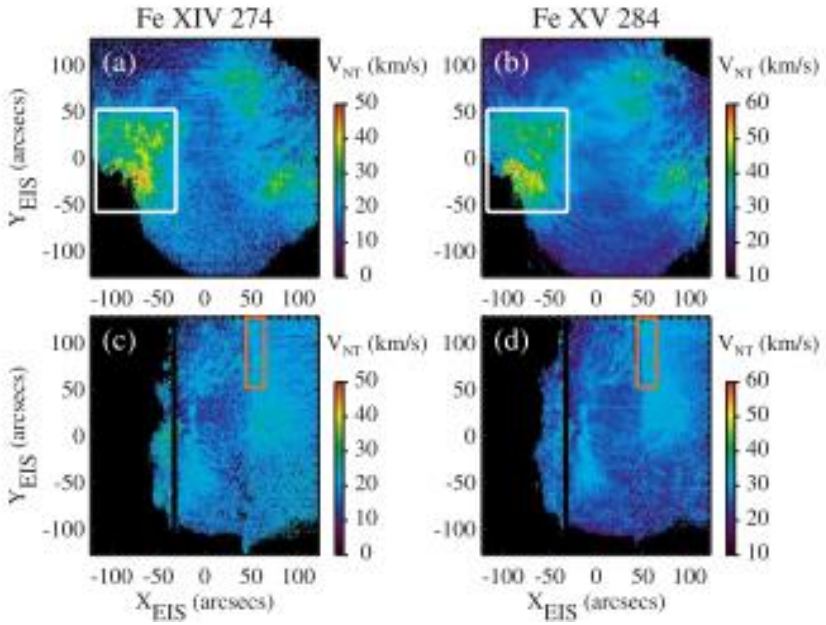

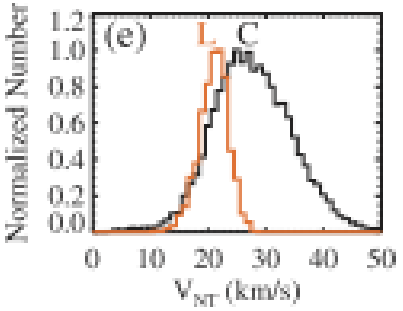

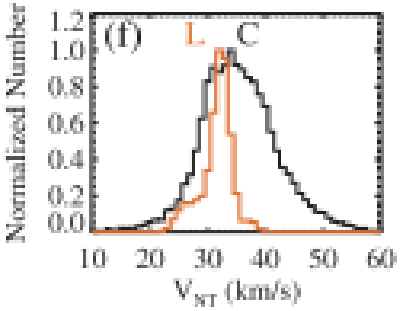

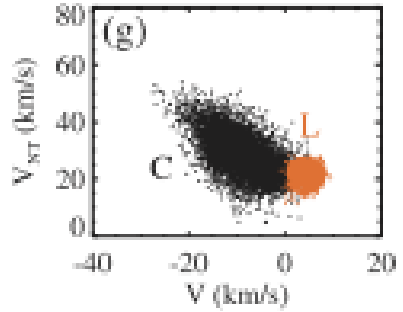

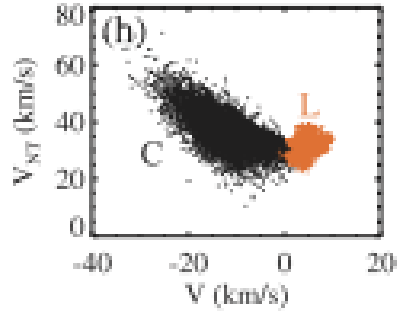

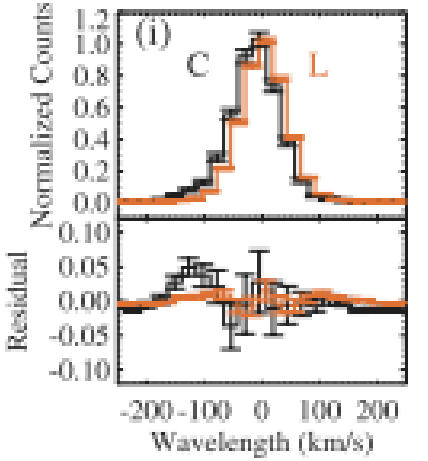

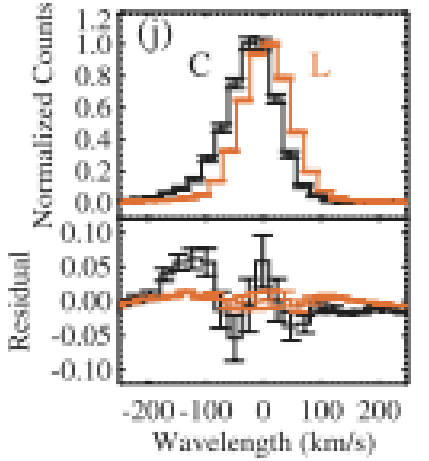

Outflows from the edge of an active region

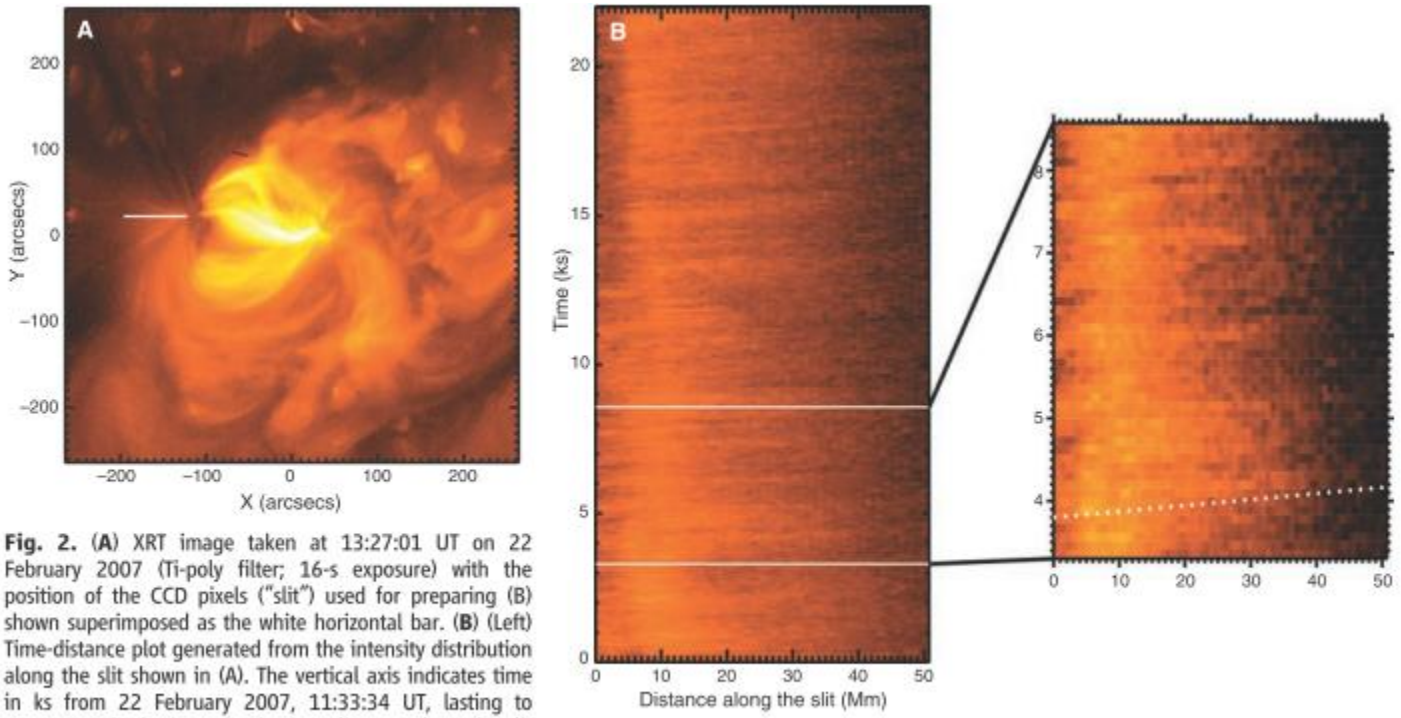

Fig. 2. (**A**) XRT image taken at 13:27:01 UT on 22 February 2007 (Ti-poly filter; 16-s exposure) with the position of the CCD pixels ("slit") used for preparing (B) shown superimposed as the white horizontal bar. (**B**) (Left) Time-distance plot generated from the intensity distribution along the slit shown in (A). The vertical axis indicates time in ks from 22 February 2007, 11:33:34 UT, lasting to 17:40 UT. The horizontal axis gives distance along the slit in Mm measured from the west (right) edge of the slit toward east (left). (Right) Expanded display for the interval indicated by the two white lines in the left image (12:28:36 to 13:56:28 UT). The dotted line represents west-to-east transverse velocity of 140 km s^{-1}.

Sakao+ 2007

- a pattern of continuous outflow of SXR emitting plasmas along open field lines
- mass loss rate that amounts to ~1/4 of the total mass loss rate of the solar wind

Outflows from the edge of an active region

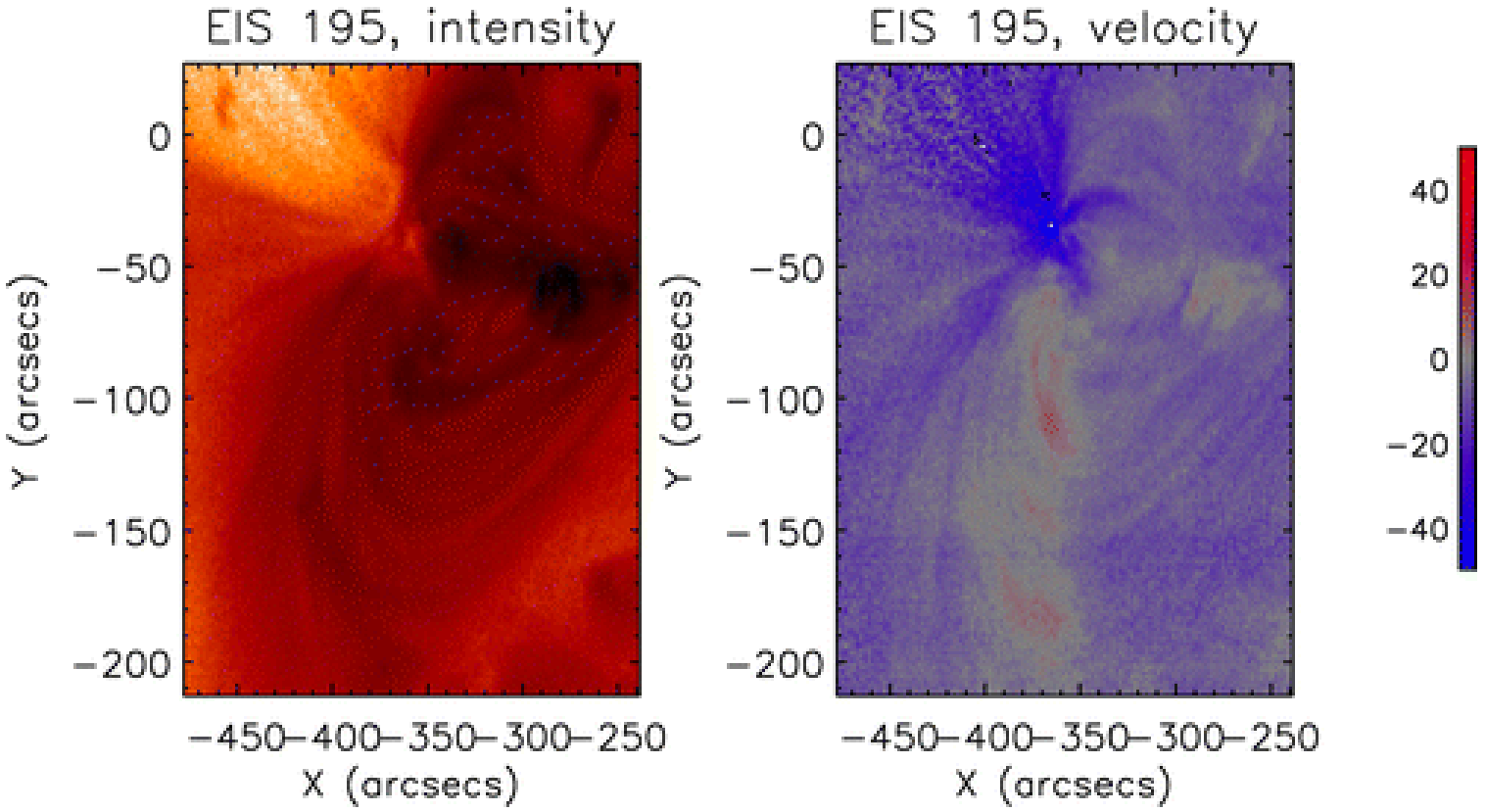

Harra+ 2008

- The Doppler velocity ranged between 20 and 50 km/s
- From the model coronal magnetic field, the outflow speeds adjusted for LOS effects can reach over 100 km/s.

High temperature active region loops

Warren+ 2011

- at the apex of the hi-temp. loops, emission measure distribution is strongly peaked near 4MK
- SXR intensity constant over 6hr
- do not show cooling loops in the core of AR
- suggest high-frequency heating scenario where heating events occur on timescales much less than a cooling time

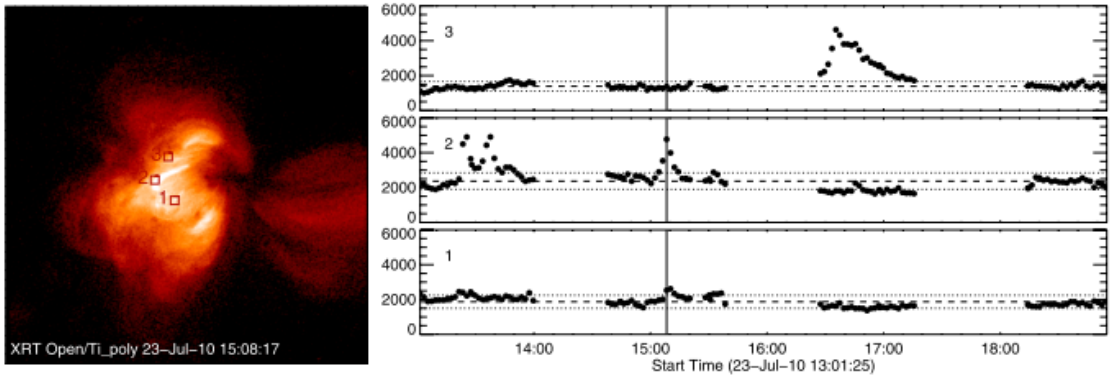

Figure 3. XRT observations of AR 11089. On the left is a frame from the observing sequence. On the right are light curves from three different locations in the core of the active region. Intensities are in DN s^{-1} $pixel^{-1}$. The dashed horizontal line is the median intensity for the period shown. The dotted horizontal lines are ±20% of the median. The solid vertical line corresponds to the time of the image. The emission in the core of the active region is relatively constant, with a variability of 20% or less. Transient events with relatively short lifetimes ($\lesssim$900 s) are also observed. The online version of the journal includes an animation of these data.

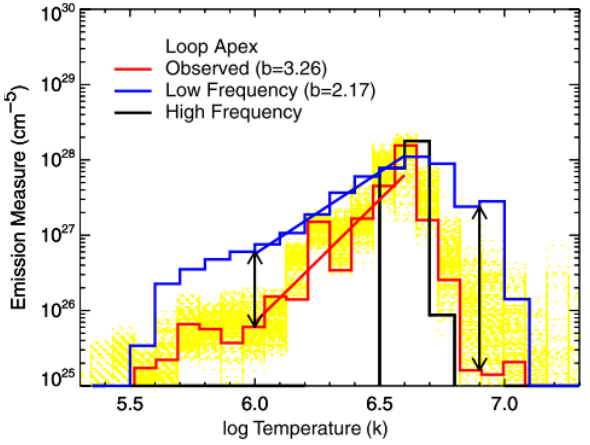

gure 7. Emission measure distributions derived from the high- and low-equency heating simulations. The distribution for both the entire loop (top nel) and loop apex (bottom panel) are shown. For comparison, our observed emission measure distribution is also shown in the bottom panel. The arrows indicate the differences between the observation and the low-frequency model at $\log T = 6.0$ and 6.9. The power-law indices (EM $\sim T^b$) are indicated for several of the emission measure distributions.

Photospheric properties of coronal loops

Kano+ 2014

- magneticfilling factor in the network is anti-correlated with the horizontal random velocity
- flux tube width of ~77 km, horizontal flow at ~2.6 km/s
- No significant difference between warm (EUV) and hot (X-ray) loops in the magnetic properties or in the horizontal random velocity at their footpoints

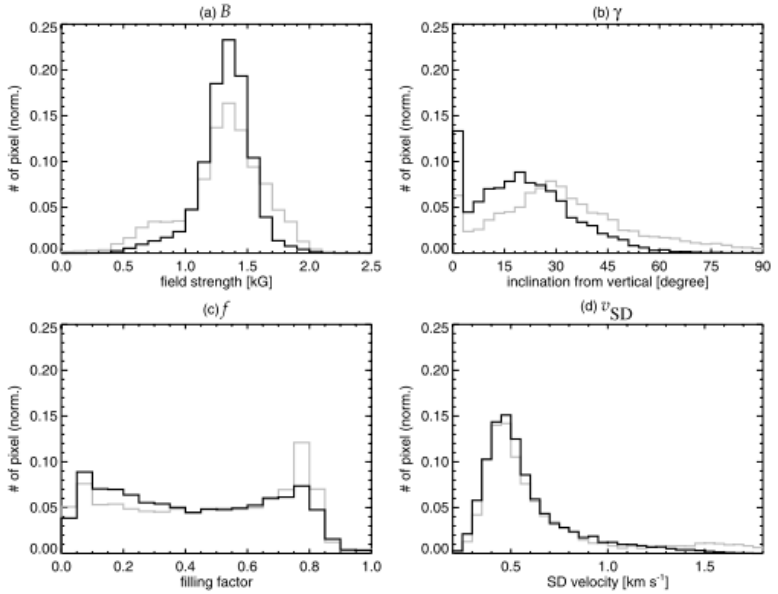

Figure 3. Histograms of photospheric properties at the footpoints located outside sunspots: (a) intrinsic field strength, (b) inclination and (c) filling factor of magnetic fields, and (d) standard deviation of horizontal velocity. Gray and black lines correspond to the footpoints of warm and hot loops, respectively.

Energy dissipation of Alfven waves in a polar coronal hole

Hahn & Savin 2013

$$F = \sqrt{\frac{\rho}{4\pi}} \langle \delta v^2 \rangle B\, A,$$

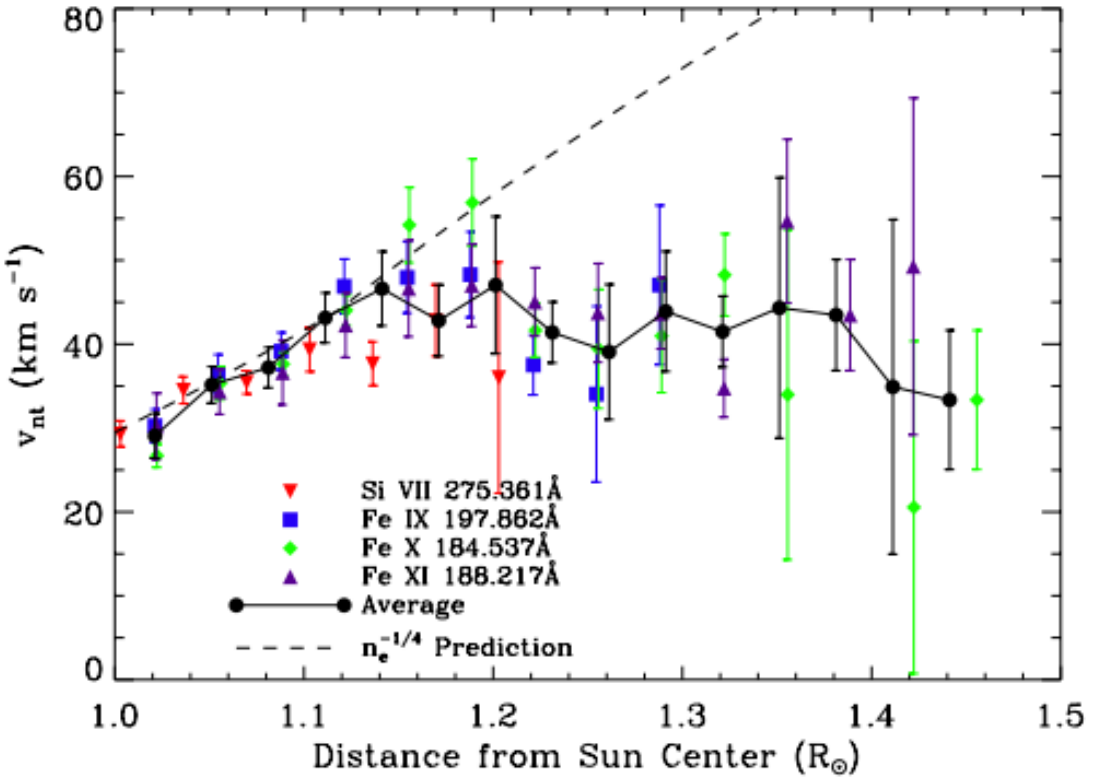

Figure 3. Symbols indicate the non-thermal velocity v_{nt} from the strongest observed lines. The filled circles and solid line show the averaged v_{nt} combining the data from the various ions. The dashed line illustrates the predicted electron density $n_e^{-1/4}$ trend for undamped waves.

Quiet corona

Warren & Brooks 2009; Brooks+ 2009

existence of universal DEM peaked near 1MK

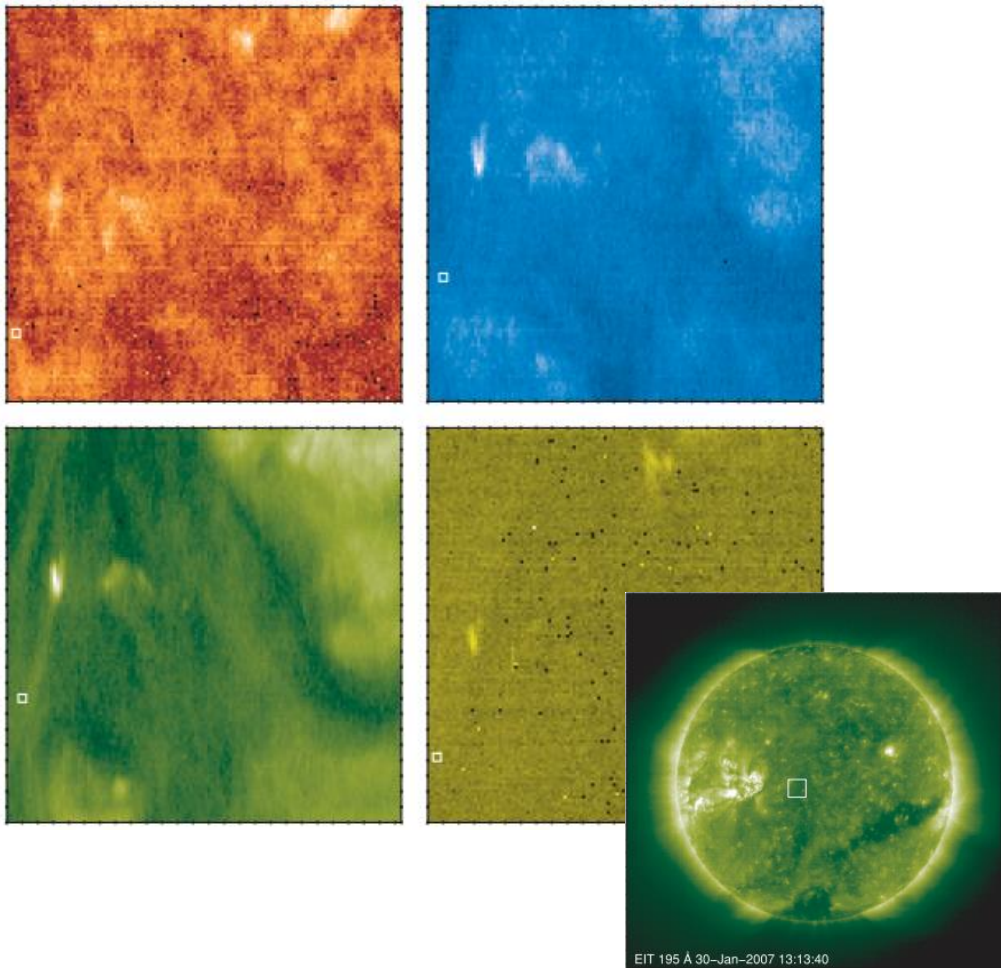

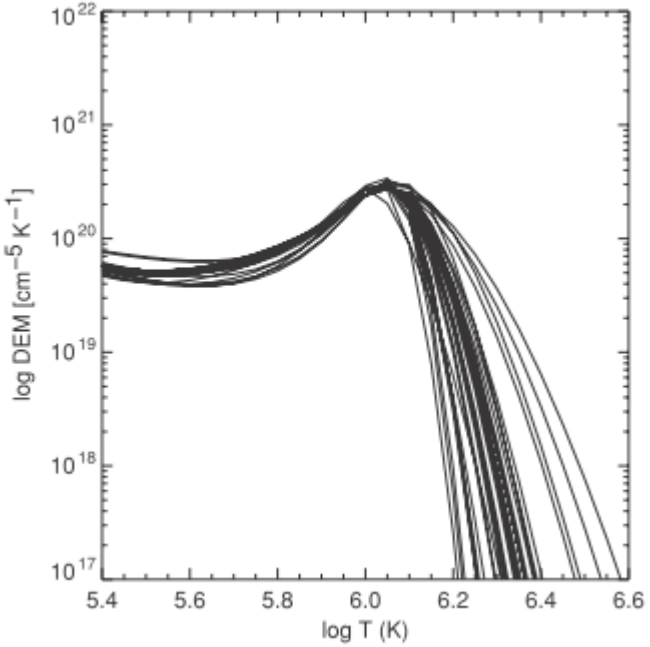

Roots of coronal heating in the chromosphere

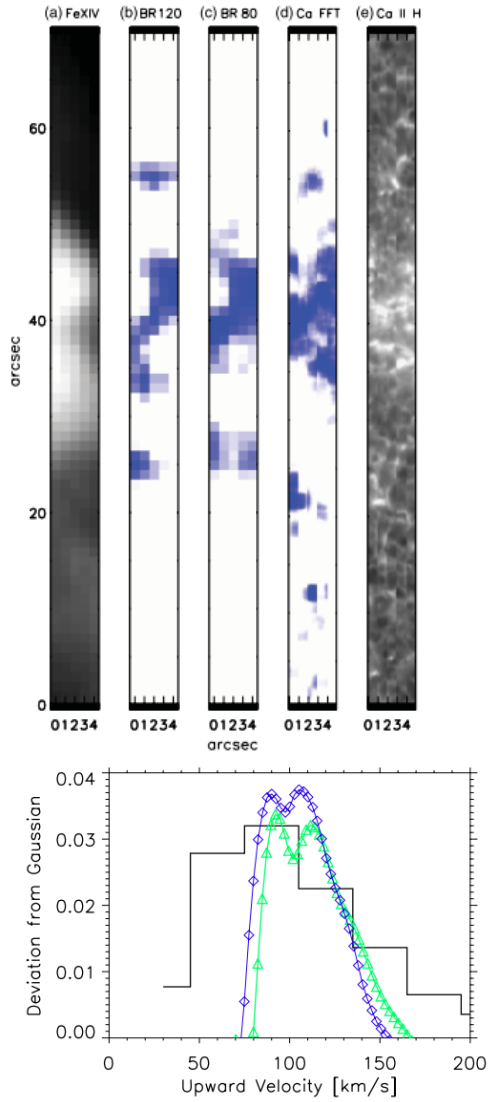

Figure 3. Histogram of upward velocities in chromospheric type II spicules (black line) as derived from Ca II H 3968 Å timeseries at the limb (from De Pontieu et al. 2007b) shows a range of velocities that is similar to coronal upflow velocities derived from subtracting a Gaussian fit from the profile of Fe XIV 264 Å (blue) and Fe XIV 274 Å (green) lines for all locations that show significant upflows in active region 10977 on 2007 December 5.

De Pontieu+ 2009

- moss regions, root of hot loops
- upflows with velocities that are similar (50-100km/s) for temperatures from 0.1 to several MK
- upflows are spatiotemporally correlated with and and have similar upward velocities as cool spicules (0.01MK)
- mass supply driven from below in the chromosphere

(c.f. De Pontieu 2011)

Chromospheric origin of heating in quiet regions ?

De Pontieu+ 2011; Mcintosh+ 2011

Ubiquitous mass supply upward by spicules and much of the plasma heated to temperatures between 0.02 and 0.1 MK and a small but sufficient plasma heated above 1MK.

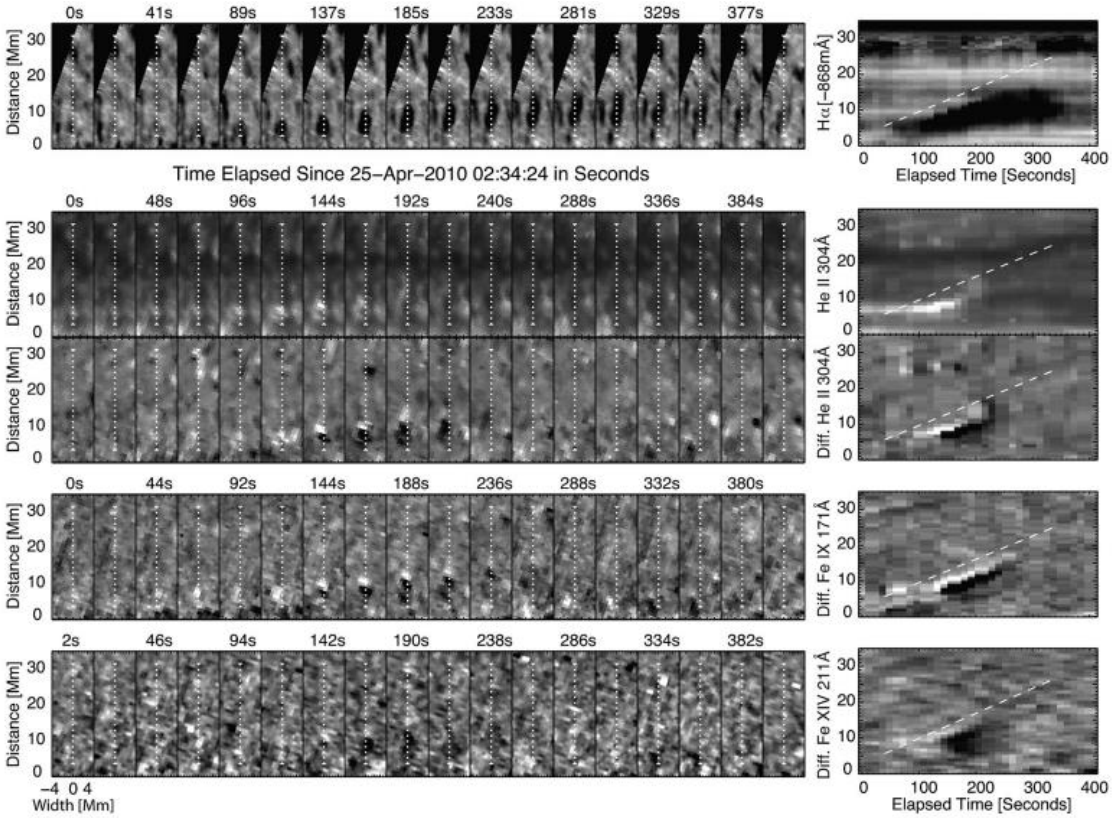

Coronal heating: summary 1/2

Active region EUV warm loops

Upflows (~ 100km/s) and line broadenings near footpoints (Hara+ 2008)

→ Nanoflare heating localrized near footpoints, Spatially unresolved

Active region X-ray hot loops

Steady in intensity, DEM peaked at 4 MK (Warren+ 2011)

→ Nanoflare heating uniformly distributed, high-frequency (w/ waiting time shorter than cooling time)

Slow solar wind

Flows from an active region edge (Sakao+ 2007; Harra+ 2008; Doschek+ 2008)

Coronal holes

Line width decay < (background electron density)^(1/4) (Hahn & Savin 2013)

→ Alfven wave heating

Fast solar wind

Mass supply by solar jets (Cirtain+ 2007); Acceleration by Alfven waves (Suzuki & Inutsuka 2005; Matsumoto & Suzuki 2012)

Coronal heating: summary 2/2

Quiet regions

Universal DEM peaked at 1MK (Brooks+ 2009) → mechanism ??? Alfven wave ? (AIA results by McIntosh+ 2011)

Mass supply from chromosphere, correlation w/ spicule activities (De Pontieu+ 2009; 2011). Proposed the chromospheric driven heating.

→ Not direct evidence, I suppose.

Relation with photospheric magnetism

No clear difference between warm and hot loops (Kano+ 2014)

→ Yet to be studied more carefully and extensively

Theory

Alfven wave heating model of coronal holes

→ Suzuki, Matsumoto model; Nonlinear generation of compressive mode and turbulent cascade

Nanoflare model

→ localization OK? Maybe no model yet.

Photospheric magnetism and flows

Horizontal magnetic flux of the quiet-Sun internetwork

Lites+ 2008

horizontal apparent flux density is 55 Mx/cm^2

vertical apparent flux density is 11 Mx/cm^2

Mag fields are organized on mesogranular scales

unresolved structures ?

(c.f. Ishikawa+ 2008; Centeno+ 2007; Orozco Suarez+ 2007; Martinez Gonzalez & Bellot Rubio 2009)

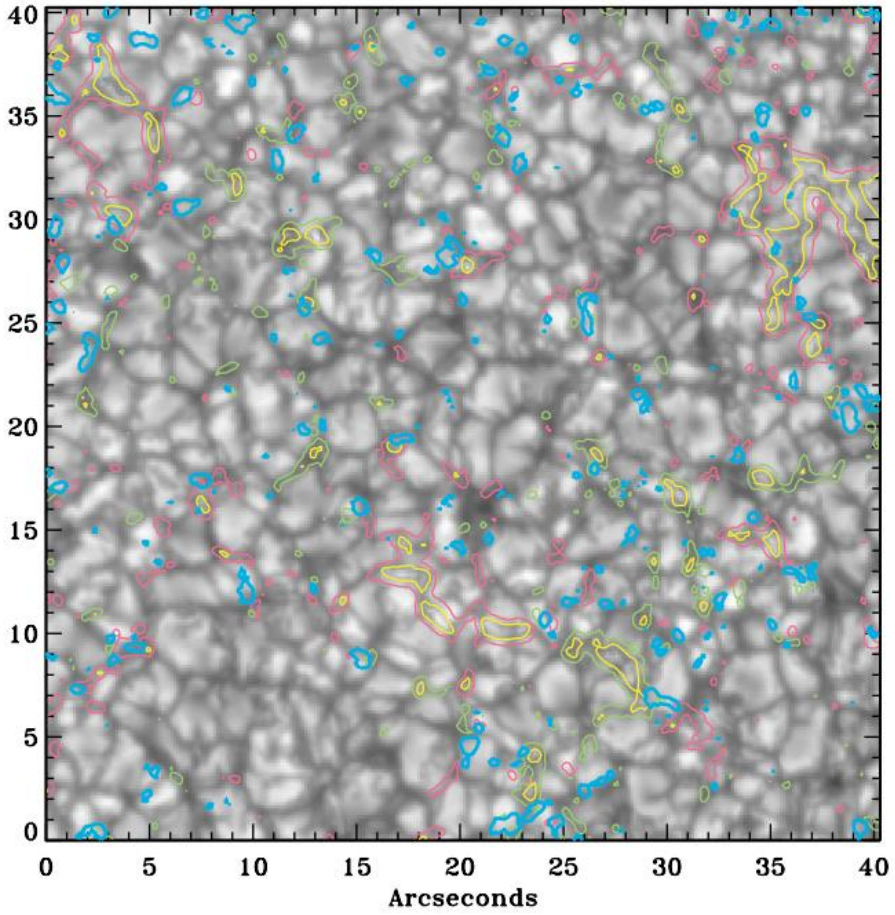

FIG. 8.—Continuum intensity for the central 40″ of Figs. 1 and 2 shown as a gray scale, with contours of B^L_{app} and B^T_{app} superimposed. Red and green contours show, respectively, the positive and negative 10 σ B^L_{app} levels (24 Mx cm^{-2}). This high threshold has been set for B^L_{app} contours to avoid cluttering the image with the very sensitive circular polarization measurements. Yellow contours are for $|B^L_{app}| = 100$ Mx cm^{-2}. Blue contours are the 3 σ B^T_{app} levels (122 Mx cm^{-2}). Note that $|B^L_{app}|$ has a strong preference for the IG lanes, that strong vertical field elements (*yellow contours*) are associated with the filigree in the IG lanes and occupy only a small fraction (<2%) of the area, and that elements of larger B^T_{app} occur away from the vertical field elements, i.e., not over the IG lanes.

Convective collapse

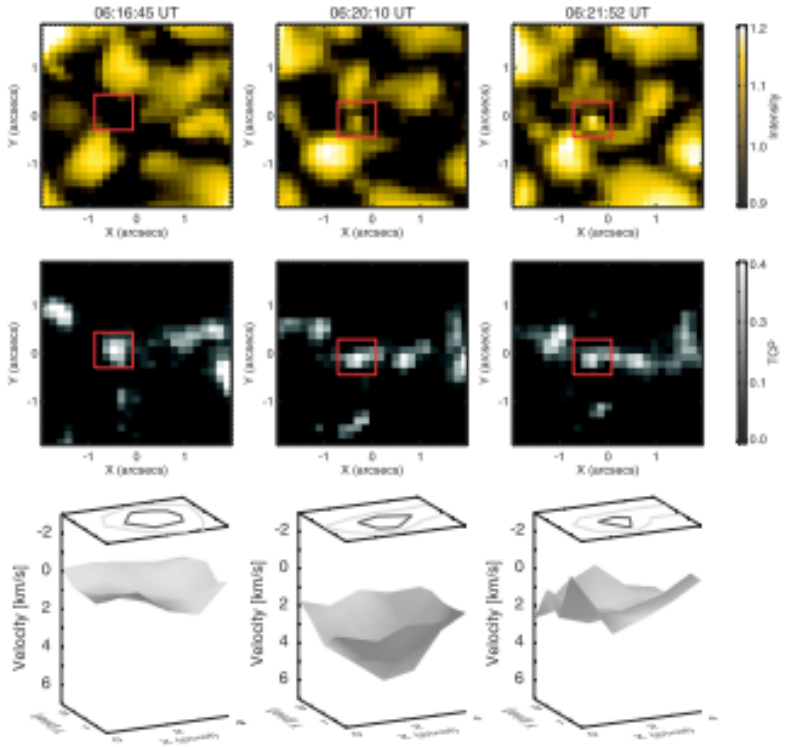

FIG. 1.—Formation of a kG field strength magnetic flux tube observed with SP. The three panels in the top row show the continuum intensity maps derived from the SP scan taken before, in the middle of, and after the formation of a kG field strength flux tube, from left to right, respectively. The red fiducial box of 0.8″ × 0.8″ (5 × 5 pixel^2) in the maps encloses the intergranular lane where the evolving flux tube of interest is seen. The middle row shows the total circular polarization (TCP) of Fe I 6302.5. Each panel corresponds to the continuum maps shown above. The bottom row shows the line-of-sight velocity and the total circular polarization in the fiducial box shown in the upper rows. The surface plot shows the velocity distribution in the fiducial box; redshifted velocity is positive. Above the surface plots the contours of total circular polarization of 0.2 and 0.3 are shown with thin and thick lines, respectively.

Nagata+ 2008

The cooling of an equipartition field strength flux tube precedes a transient downflow reaching 6 km/s and intensification f the field strength to 2 kG.

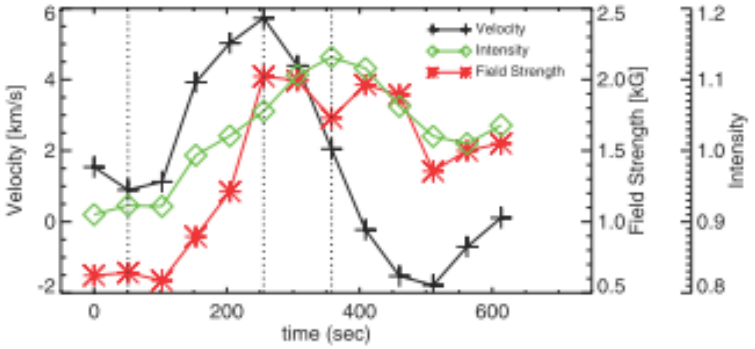

FIG. 3.—Evolution of the velocity, continuum intensity, and field strength observed at the center of the evolving flux tube. The physical parameters are extracted from the central pixel of the magnetic feature with a growing bright point. The black line with pluses represents the line-of-sight velocity derived from the Fe I 6302 Stokes *V* profile. The green line with diamonds represents the normalized continuum intensity. The red line with asterisks represents the magnetic field strength derived from the Milne-Eddington inversion for the observed profiles. Three dotted vertical lines represent the times when the scans shown in Fig. 1 were made. The start time is 2007 February 6 06:15: 54 (UT).

Polar magnetic fields

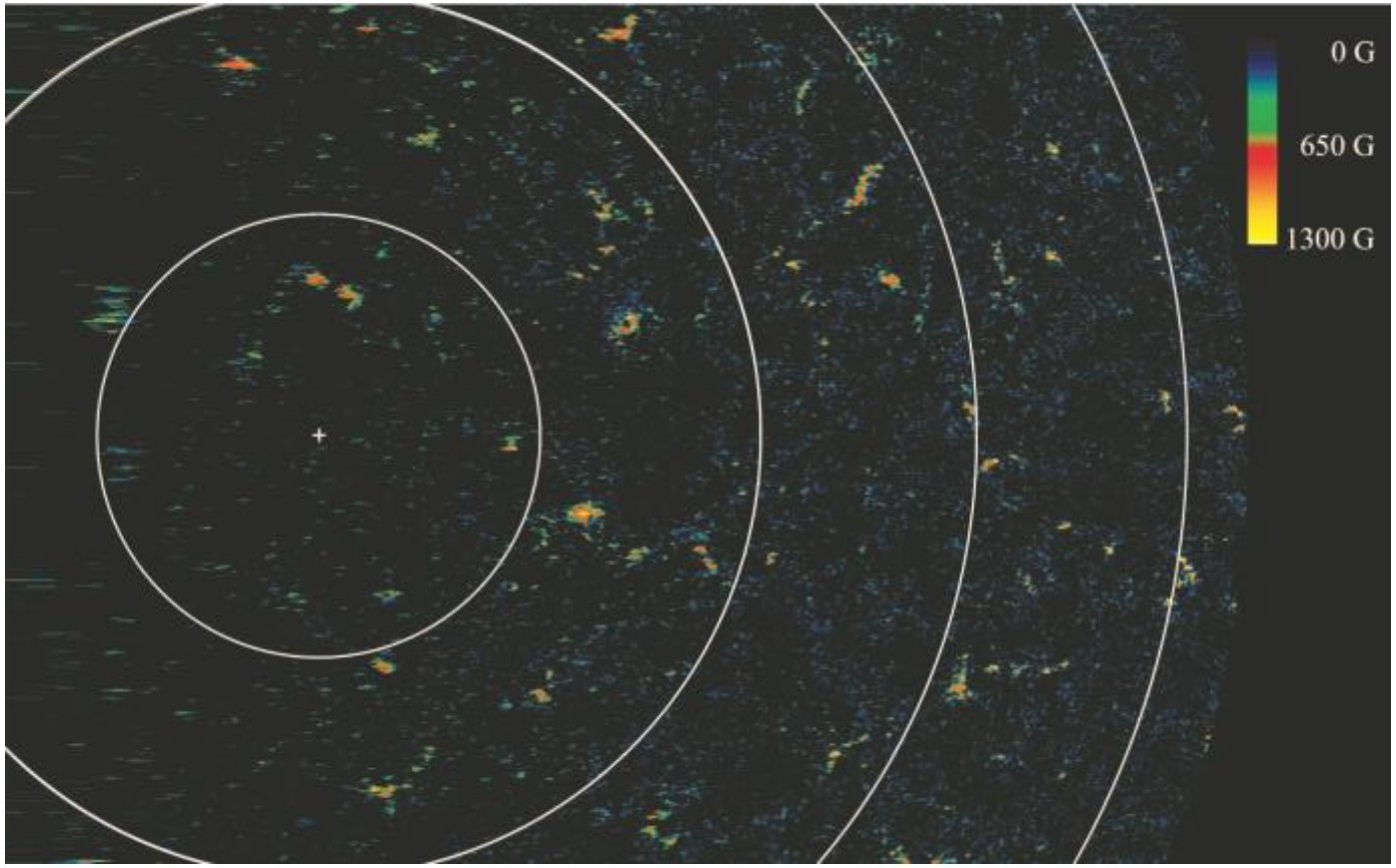

Tsuneta+ 2008

- Vertically oriented magnetic flux tubes with field strengths as strong as 1kG
- ubiquitous horizontal fields

Power spectra of V & B on the photosphere

Katsukawa & Orozco Suarez 2012

kinetic and thermal spectra have a prominent peak at the granular scale while the magnetic one have a broadly distributed distribution

The power-law indices of the mag. power spectra are close to or smaller than -1, which suggests the total mag. energy mainly comes from either the granular scale mag. structures or both the granular and smaller ones contributing evenly.

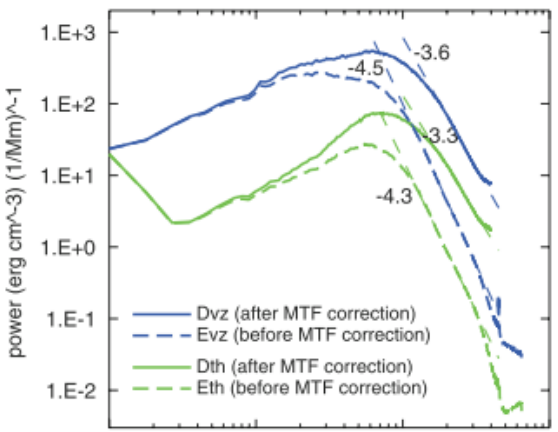

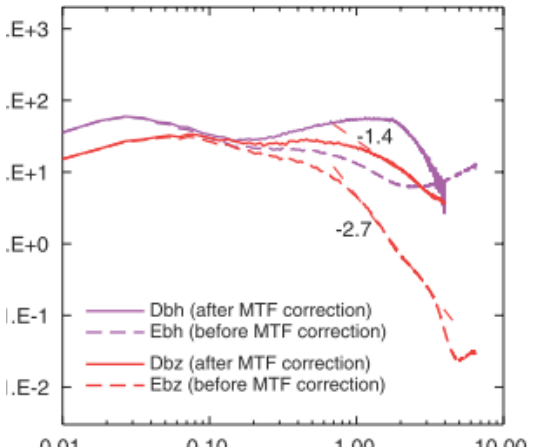

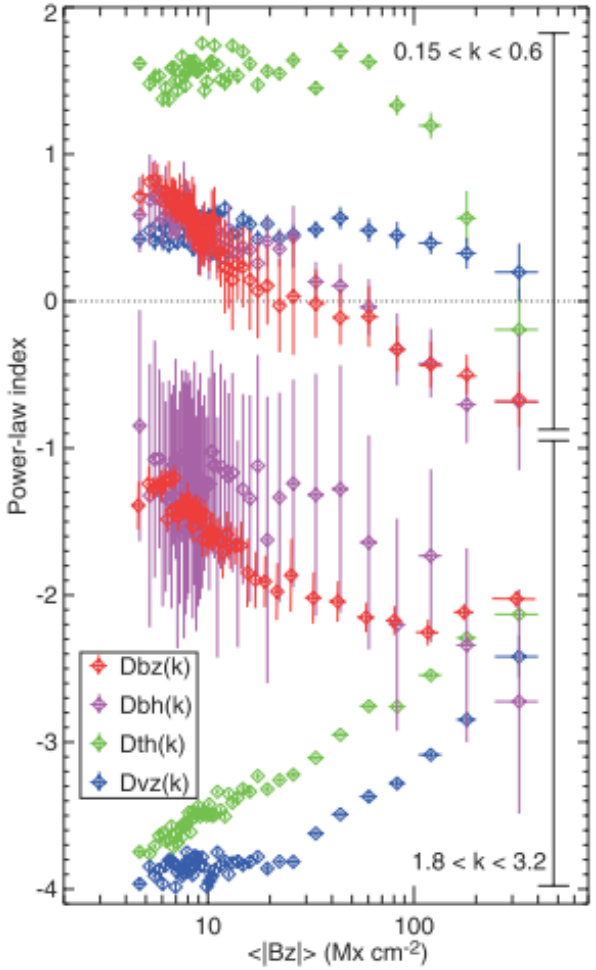

Figure 6. Power-law indices α of the power spectra as a function of the averaged density of unsigned flux $\langle|B_z|\rangle$. The power-law indices are obtained in two wavenumber ranges, between $k = 0.15$ and 0.6 Mm^{-1} (corresponding to the scale larger than granules) and between $k = 1.8$ and 3.2 Mm^{-1} (corresponding to the scale smaller than granules). The green, blue, red, and purple symbols represent the power-law indices of $D_{th}(k)$, $D_{b_h}(k)$, $D_{b_z}(k)$, and $D_{bb}(k)$, respectively. The vertical error bars show the $\pm 1\sigma$ range of the power-law indices when we take into account the variation of the power spectra in each $\langle|B_z|\rangle$ interval.

Magnetic cancellation in a quiet region

Iida+ 2010

Transverse magnetic field connecting the canceling mag. features and strong long-lasting Doppler redshift signal are found.

Consistent with Omega-loop submergence

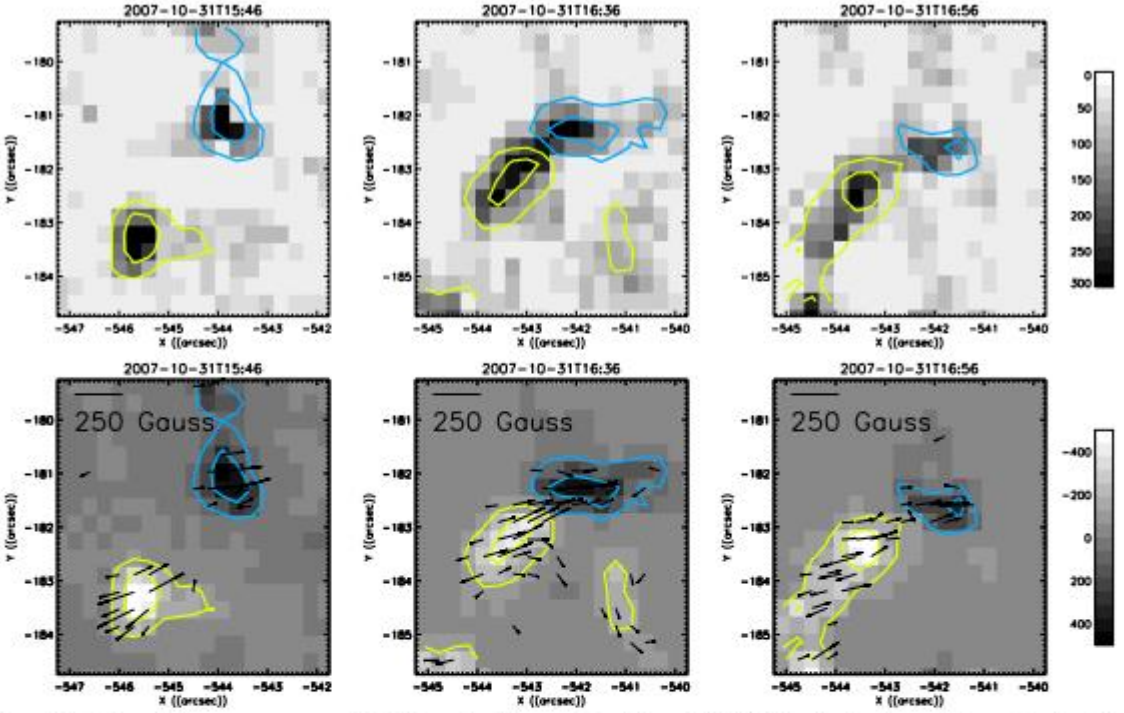

ngth and direction of the transverse magnetic field in unit of Gauss obtained from SOT/SP. Top: the background shows the strength ellow/blue contours are positive/negative LOS magnetic field. The counters show ±100 G and ±300 G. Bottom: the white/black ba ive LOS magnetic field. The arrows show the direction of the transverse field. The contours show the same strength as the top panels. ıity in the transverse field direction.

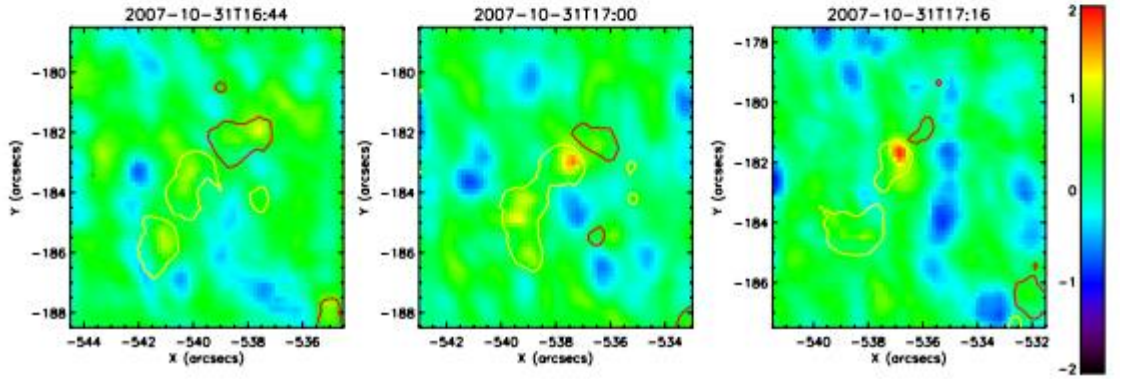

Supergranulation alignment in polar regions

Nagashima+ 2011

Helioseismology by SOT

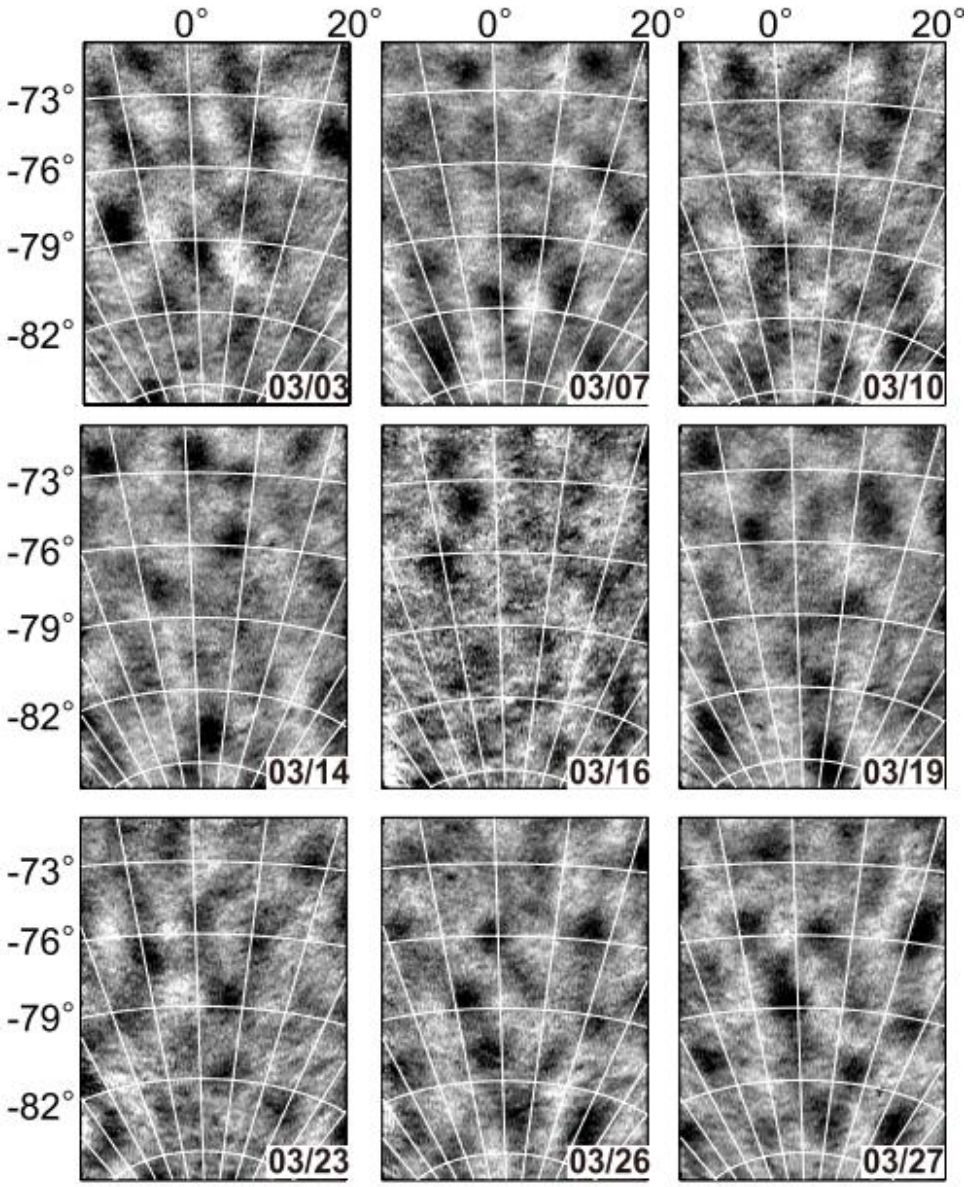

Photospheric magnetism and flows: summary

Magnetic flux in quiet regions

Dominant horizontal flux (Lites+ 2007; Ishikawa+ 2008; Centeno+ 2007; Orozco Suarez+ 2007; Martinez Gonzalez & Bellot Rubio 2009)

→ surface dynamo ? (Schuessler & Voeggler 2008)

Formation of intensive magnetic tubes

Downflow and intensification: evidence of the “convective collapse” (Nagata+ 2008)

Polar fields

kilo-Gauss patches, dominance of horizontal field (Tsuneta+ 2008) and its reversal (Shiota+ 2012)

→ information for global dynamo ?

Photospheric magneto-convection

Dependence of power-law spectra difference between B & V. Flat B spectrum with power-law index ~ -1. (Katsukawa & Orozco Suarez 2012)

→ suggest surface dynamo and even contribution or dominance of small scale magnetic field

And...

Emerging flux (e.g. Cheung+ 2008), cancellation (Iida+ 2010), filament formation (Okamoto+ 2008)

Local helioseismology (Nagashima+ 2011)

Table of contents

Overview of Hinode results & What to do next.

- Chromospheric dynamics
- Flares: flows and triggers
- Coronal heating and solar wind
- Photospheric magnetism and flows

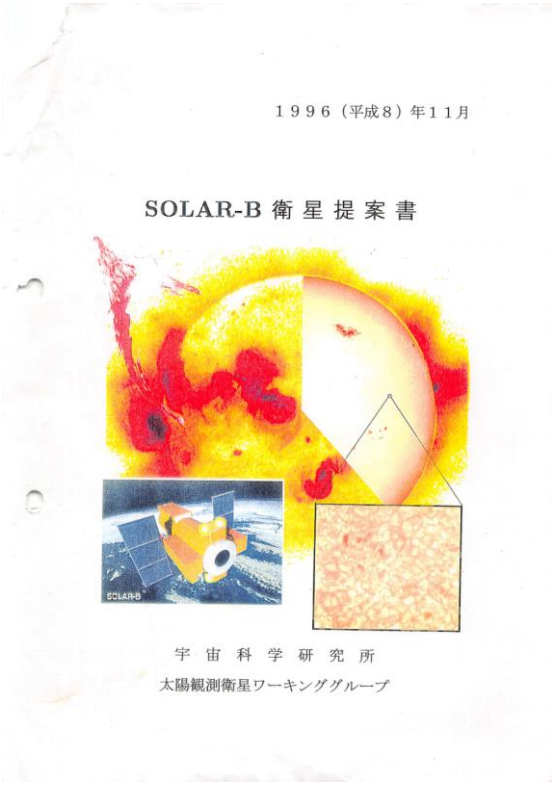

SOLAR-B衛星提案書1996年11月

挑戦する研究課題

- 外層大気（コロナ・彩層）の加熱メカニズム
- 太陽磁場の基本構造としての微細磁束管とダイナモ機構
- コロナのダイナミックスとリコネクションの詳細究明

What to do next ?

Chromospheric dynamics

spicules: generation, thermalization, waves ...

Flares and coronal activities

reconnection: shocks (do not exist ?)

trigger: proposed model's generality, formation of active regions, emerging flux, connection w/ below the surface

micro-, nano-flares, non-thermal aspects

NLFFF model using chromospheric mag. field

Coronal heating

Almost done, I suppose...

Relation with the energy input from the lower atmosphere

Mechanisms for quiet region heating are still open.

Theory needs for localized nano-flares at footpoints.

Photospheric magnetism and flows

...

What's further ?

Solar-C がんばりましょう

Science setups

Radiative MHD: non-LTE, partially ionized ...

Preparation for the further future:

Solar dynamo

Helioseismology

Link with

- planet systems, not only solar one
- other stars, young Sun

End